Exploring Return Dynamics via Corridor Implied Volatility

Torben G. Andersen
Kellogg School of Management, Northwestern University

Oleg Bondarenko
Department of Finance, University of Illinois at Chicago

Maria T. Gonzalez-Perez
CUNEF, Madrid

Some fundamental questions regarding equity-index return dynamics are difficult to address due to the latent character of spot volatility. We exploit tick-by-tick option quotes to compute a novel "Corridor Volatility" index which may serve as an observable proxy for short-term volatility. Exploiting this index, we find that equity-index volatility jumps are common, symmetrically distributed, and cojump with the underlying returns. Moreover, the return-volatility asymmetry is more pronounced than is generally recognized and is in force for both diffusive and jump innovations in volatility. Finally, the index performs admirably during turbulent market conditions, constituting a useful real-time gauge of market stress. (*JEL* G13, C58)

Introduction

The characterization of the equity-index return dynamics has been refined in recent decades with the growing access to daily and subsequently tick-by-tick financial price data; yet much remains unresolved. We now recognize that returns have time-varying means, they display very persistent volatility fluctuations, market prices occasionally move abruptly, that is, "jump," and return and volatility innovations are negatively correlated. We are coming to

Elements of this work were previously included in the working paper entitled "Coherent Model-Free Impled Volatility: A Corridor Fix for High-Frequency VIX." Andersen acknowledges support from CREATES, Center for Research in Econometric Analysis of Time Series, supported by the Danish National Research Foundation (DNRF78). Gonzalez-Perez gratefully acknowledges financial support from the Ministerio de Economia y Competitividad, Spain (MEC Research Project ECO2012-32554). We thank Kris Jacobs, Jesper Lund, and seminar participants at the European Finance Association Meeting, Copenhagen, August 2012, the 2012 Western Finance Association Meeting, Las Vegas, the 2011 Osaka Conference on "High-Frequency Data Analysis in Financial Markets," the Midwest Econometrics Group 2011 Meetings at the University of Chicago, the Federal Reserve Board of Governors, the SoFiE-CREATES 2010 Conference in Aarhus, the University of Illinois at Chicago, Virginia Tech, Spot Trading, the Wisconsin School of Business, and the Illinois Institute of Technology for comments. Send correspondence to Oleg Bondarenko, Department of Finance, University of Illinois at Chicago, 601 S. Morgan St., Chicago, IL 60607. E-mail: olegb@uic.edu.

doi:10.1093/rfs/hhv033 Advance Access publication June 1, 2015

grips with the fact that return volatilities jump as well, and, indeed, volatility and returns may jump simultaneously, that is, "cojump." Nevertheless, the origin, interaction, and propagation of these effects from the highest intraday frequencies to the observed fat-tailed and asymmetric return distributions at longer horizons remain elusive. The main obstacle for progress is the lack of high-frequency observations on the latent spot volatility process. Even though there is a literature establishing procedures for consistent extraction of spot volatility from high-frequency asset returns, such estimates are too imprecise to allow for identification of the timing and size of volatility jumps or the computation of spot return-volatility correlations.

In this paper, we exploit a novel corridor implied volatility index, CX, to uncover new features of the equity-index return dynamics. Most importantly, we document that volatility jumps are more prevalent than typically acknowledged. Moreover, although the jump intensity fluctuates, the jumps are fairly uniformly distributed across time, and there is no strong serial correlation in the jump direction. In addition, we find the volatility jump distribution to be symmetric, so negative volatility jumps are as common as positive ones. This holds true also for the periods characterized by escalating volatility and dramatic drops in equity prices, such as the height of the financial crisis or the European sovereign debt crisis. This contrasts sharply with standard asset pricing models that typically allow only for positive volatility jumps and often explicitly preclude negative volatility jumps. Our finding is very robust. In fact, we find equity volatility to cojump with the equity-index returns, and these simultaneous jumps are highly negatively correlated. Hence, large upward price revisions are usually accompanied by dramatic drops in volatility and vice versa.

We also find the general contemporaneous return-volatility relation, or leverage effect, to be strongly negative with a typical correlation between return and volatility innovations of about -0.85, which is a substantially stronger effect than reported in the extant literature. There are numerous sources of noise in standard volatility series that tend to bias empirical estimates toward zero, so this discrepancy may be explained by the improved accuracy afforded by our new CX index. Importantly, we find the leverage effect to be similar for regular (small) volatility innovations and for volatility jumps. Hence, the return-volatility asymmetry applies equally to the diffusive and jump components of the return and volatility processes. We further document significant time variation, with the correlation turning decidedly more negative when markets are turbulent. This suggests that returns and volatilities become increasingly negatively correlated during adverse and uncertain economic conditions. These are also times of elevated variance risk premiums, thus potentially linking our results to systematic movements in the pricing of equity risk over the economic cycle.

Finally, relative to the widely adopted VIX index, our CX index provides a vastly improved indicator of evolving market conditions during periods of

unusual stress. In an illustration to the flash crash, we identify large systematic biases in the VIX index, which are greatly alleviated if we instead rely on the CX index as a proxy for the evolution in short-run volatility. As such, the real-time transmission of a robust corridor implied volatility measure to the marketplace would enhance information flow and transparency during stressful episodes, benefiting market participants, exchanges, and regulators alike.

The key development enabling our analysis of the high-frequency equity-index return dynamics is the construction of our high-frequency CX volatility series. Like the VIX, it is a model-free implied volatility measure obtained from quotes for a wide cross-section of options. However, it employs a consistent truncation rule that ensures the liquidity of the underlying options and coherence of the associated return variation measure across time. This is critical for applications that are sensitive to high-frequency features of the volatility series. Effectively, we use innovations in the CX series as a proxy for innovations in spot volatility. This raises important issues, as CX is derived from short-term options rather than from the actual spot volatility. Hence, our CX series will also reflect the pricing of equity volatility over nontrivial time intervals. Consequently, we undertake a variety of robustness checks to gauge whether the properties of the CX innovations provide a good approximation to the corresponding features of spot volatility.

We provide a number of theoretical contributions as well. We cast the entire class of model-free implied volatility measures within the overarching framework of corridor volatility indices. The standard measures are encompassed as special cases that arise for infinite barriers. In this context, we adopt the perspective of Bondarenko (2014) in demonstrating robustness of the model-free return variation concept to both price jumps and discrete sampling of the underlying price observations. In particular, we characterize the payoff structure for corridor variance swaps when jumps induce a breach of the barriers. This issue is unique to our more general corridor setting but is essential for our applications. Finally, we develop a new mechanism for determining the barriers that ensure an economically consistent truncation point for the option strike range, when constructing the CX measure. This procedure relies only on observable option prices and is thus truly model-free, in contrast to earlier implementations that tied the barriers to the at-the-money Black-Scholes implied volatility.

It is critical for our applications that the exact pricing result for the (corridor) return variation, obtained via the CX measure, is robust to jumps and discrete sampling. Those properties have been scrutinized in the recent literature, as they fail for standard definitions of returns. The crucial step in our theoretical development is to apply the notion of return variation to asset returns defined through a suitable linear combination of arithmetic and continuously compounded returns. Not only does this imply exact pricing of return variation but it also provides an extremely accurate approximation for a weighted average of standard realized volatility measures. As such, our results render the

inconsistencies in the model-free valuation of return variation in the presence of price jumps, laid out by, for example, Martin (2012), inconsequential.

Our paper relates to a vast empirical literature on the return dynamics in general and volatility jumps, leverage effects, and real-time volatility indicators in particular. Insistence on including both return and volatility jumps in asset pricing models at the daily level goes back at least to Eraker, Johannes, and Polson (2003). For intraday data, the literature is much more recent, see, for example, Jacod and Todorov (2010). Amengual and Xiu (2014) price downward volatility jumps, extracted from a parametric model for daily returns and relate these jumps to the resolution of policy uncertainty. The estimation of the leverage effect from high-frequency data is only emerging, with examples including Aït-Sahalia, Fan, and Li (2013) and Kalnina and Xiu (2014). Finally, the use of CX as a real-time gauge of market conditions relates to the recent literature on potential warning signals for market turmoil, see, for example, Easley, de Prado, and O'Hara (2012) and Andersen and Bondarenko (2015).

1. Model-free Return Variation Measures

A rapidly expanding literature relies on the model-free option-implied return variation measure, as reviewed in, for example, Britten-Jones and Neuberger (2000), for gauging the expected return volatility and analyzing the variance risk premium dynamics. Conveniently, the VIX measure, based on S&P 500 equity-index options and disseminated almost continuously during exchange trading hours by the Chicago Board of Options Exchange (CBOE), is constructed in accordance with this notion.

However, there is increasing concern that the VIX measure is not truly model-free. While Jiang and Tian (2005) and Carr and Wu (2009) conclude that jumps are unlikely to create sizable biases, this view has been revised in the wake of the financial crisis, see, for example, Carr, Lee, and Wu (2012). In addition, Martin (2012) cites the vanishing over-the-counter variance swap market for individual stocks in arguing that the alternative simple volatility index, or SVIX, is preferable. The problem is that price jumps induce a discrepancy between the fair pricing of future cumulative squared returns and VIX^2, even in the continuous sampling limit. This is true whether we consider simple (arithmetic) or log (continuously compounded) returns. Both return definitions have used in practice to compute the payoff on volatility contracts. Unfortunately, they imply different valuation formulas that both deviate from VIX^2 in pricing jumps, further fueling the uncertainty regarding the validity and reliability of the notion of model-free return variation in general settings.

In contrast, we summarize recent results establishing what exact concept of return variation is priced by the VIX, and we argue that this theoretically is fully satisfactory. That is, we reinstate model-free implied volatility as a meaningful measure for the expected future risk-neutral return variation. Moreover, we point out that this notion is consistent with discrete sampling so it applies to

existing variance swap contracts whose payoffs are determined by discretely sampled squared returns (empirical realized volatility measures). Moreover, it allows for exact replication and hedging in discrete time. In short, we argue that the theory behind the VIX is both relevant and resilient.

Subsequently, we highlight a separate practical concern. The option strike range required for computing VIX is, by necessity, finite and must be truncated relative to the theoretical prescription. This biases the measure downward. In addition, it induces idiosyncratic variation in the metric unless the truncation is chosen according to a coherent criterion over time. In response, we turn to the concept of corridor implied volatility, which captures only a specific component of the overall return variation. We extend the theory above to characterize the exact notion of realized return volatility captured by the corridor implied volatility metric in a setting with price discontinuities and discrete sampling.

1.1 The basic setup

Throughout this section we fix the current time at $t=0$ and focus on a frictionless and arbitrage-free setting with continuous trading in a risky and risk-free asset over the period $t \in [0, \mathbb{T}]$. We further assume a rich set of derivatives securities written on the underlying asset are traded. Specifically, there is a futures contract with expiration at date T_F, with $0 < T_F \leq \mathbb{T}$. In addition, there are a continuum of European-style options written on the futures contract with expiration at T, where $0 < T < T_F$. The available strike prices K cover the full support of the futures price, that is, the positive real line. We denote the futures price at time t by F_t, while $P_t(K) = P(K, T; F_t, t)$ and $C_t(K) = C(K, T; F_t, t)$ are the prices of European put and call options with strike K and tenor T. Moreover, it is convenient to define $M_t(K) = \min(P_t(K), C_t(K))$ as the minimum price of the put and call with strike K. In other words, of the two vanilla options with strike K, $M_t(K)$ is the price of the one that is currently out-of-the-money.

The price processes are defined on a complete, filtered probability space $\left(\Omega, \mathscr{F}, \mathbb{P}; \mathscr{F}_{t\in[0,\mathbb{T}]}\right)$, and they will, under standard no-arbitrage conditions, constitute semimartingales with respect to the filtration $\mathscr{F}_t$. Hence, the futures price has a general jump-diffusive representation,

$$\frac{dF_t}{F_t} = \mu_t dt + \sqrt{v_t} dW_t + \kappa_t dJ_t, \tag{1}$$

where W_t is a Wiener process under $\mathbb{P}$, J_t equals one if there is a jump at time t and zero otherwise. The jump return, κ_t, is nonzero only when $J_t = 1$, which is governed by the finite jump intensity λ_t; that is, the price jumps are of finite activity. The drift μ_t, spot variance v_t, and jump characteristics (λ_t, κ_t) are adapted to the filtration $\{\mathscr{F}_t\}_{0\leq t\leq \mathbb{T}}$, so they evolve stochastically. Finally, λ_t is finite; that is, the price jumps are of finite activity. In this setting, there exists an equivalent martingale, or "risk-neutral," measure, $\mathbb{Q}$, for which the futures price constitutes a martingale with respect to $\mathscr{F}_{t\in[0,\mathbb{T}]}$. The risk-free rate plays

no direct role in our theoretical exposition, so we set it to zero.[1] Throughout this section, we fix the interval $[0, T]$ and define the integrated variance as

$$IV \equiv \int_0^T v_u \, du. \tag{2}$$

Further, we let $\mathcal{T} = \{t_0, t_1, \ldots, t_n\}$ denote a sampling partition with trading dates $0 = t_0 < t_1 < \ldots < t_n = T$ and let $\Delta t = \max_i (t_i - t_{i-1})$. There are no other restrictions on the partition. In particular, trading dates do not have to be equidistant, Δt does not have to be small, and the partition could consist of as little as a single interval, that is, $n = 1$.

Finally, the CBOE VIX approximates the square root of the so-called model-free implied volatility,

$$MFIV = 2 \int_0^\infty \frac{M_0(K)}{K^2} \, dK. \tag{3}$$

One theme of this paper is to develop procedures for approximating measures related to the risk-neutral expected return variation. The usual approach is to rely on the squared VIX as a proxy, because MFIV $= E^{\mathbb{Q}}[IV]$, if the price follows a pure diffusion. However, this metric is widely perceived to be flawed when the price process is discontinuities, see, for example, Carr, Lee, and Wu (2012) and Martin (2012). Thus, we first review existing theoretical results for the MFIV measure, which, in turn, guides us toward new ways to improve the measurement of model-free implied volatility.

1.2 Which notion of return variation is priced by the VIX?

As noted, there is controversy regarding the usefulness of the MFIV formula when the price path is discontinuous. The issue arises, in part, due to the fact that the magnitude of price jumps differs depending on the return definition. For example, using the sampling partition $\mathcal{T}$, we can consider two returns over $[t_{i-1}, t_i]$: the continuously compounded, or log-return $r_i^c = \ln(F_i) - \ln(F_{i-1})$, and the simple or arithmetic return $r_i^s = (F_i - F_{i-1})/F_{i-1}$, where F_i denotes the price at time t_i. The corresponding realized volatility measures are then defined as

$$RV^c \equiv \sum_{i=1}^n \left(r_i^c\right)^2 \qquad \text{and} \qquad RV^s \equiv \sum_{i=1}^n \left(r_i^s\right)^2. \tag{4}$$

If the prices are generated by a pure diffusion, then both $RV^c \to IV$ and $RV^s \to IV$ as $\Delta t \to 0$. This suggests that sensible approximations to the return

[1] In reality, the risk-free rate is nonzero, of course. Hence, in the empirical work, we convert spot option prices into forward prices (for delivery at date T) by multiplying the spot prices by e^{rT}, where r is the risk-free rate over $[0, T]$.

variation may be derived from both the log and simple returns.[2] However, whenever the prices jump by a significant amount, nontrivial discrepancies arise between the two return definitions. In fact, the MFIV prices neither the limiting quadratic return variation of the log nor the simple returns.[3]

Consequently, we may ask: what type of return variation, if any, does the model-free option implied volatility price in the general case? To convey the answer, we require additional notation. Define the squared "weighted" return $(r_i^w)^2 = 2\left(r_i^s - r_i^c\right)$. Despite the unconventional appearance, this definition does capture the size of squared returns as one may show, by direct computation, that

$$\left(r_i^w\right)^2 = \frac{2}{3}\left(r_i^c\right)^2 + \frac{1}{3}\left(r_i^s\right)^2 + O\left(\left(r_i^c\right)^4\right). \tag{5}$$

This implies that $(r_i^w)^2$, to an extremely good approximation, represents a weighted average of the log and simple squared returns. We define the corresponding notion of realized variance as

$$RV^w \equiv \sum_{i=1}^{n}\left(r_i^w\right)^2 \approx \frac{2}{3}RV^c + \frac{1}{3}RV^s. \tag{6}$$

Both log and simple squared returns are used as the basis for variance swap contracts. Equation (5) defines a quantity falling strictly in-between these standard notions, meaning it inherits the general intuition and properties associated with a squared return. As shown below, in practice, this also implies a very close relation between the realized volatility RV^w and the corresponding weighted average of the RV obtained from log and simple returns, as stipulated in Equation (4). To provide some intuition, Appendix A.2 contrasts the three definitions of the realized variance in the continuous-time limit.

The notion of realized volatility introduced in Equation (6) is motivated by the following remarkable model-free option implied variance pricing result, derived in Bondarenko (2014).

Proposition 1. For any partition $\mathcal{T}$, MFIV reflects the fair valuation of RV^w. That is,

$$E_0^{\mathbb{Q}}[RV^w] = \text{MFIV} = 2\int_0^{\infty}\frac{M_0(K)}{K^2}dK. \tag{7}$$

The proposition has two striking implications. First, even in the presence of jumps, the MFIV prices the expected future return variation correctly. In other words, the theoretical VIX formula is jump robust, as long as the squared returns are measured by $(r_i^w)^2$. Second, the formula applies also for the pricing

[2] Indeed, over-the-counter variance swaps are traded using either notion of returns as the basis for the payoff.

[3] This is, of course, well recognized in the literature, see, for example, the exposition in Carr and Wu (2009). This fact is exploited as the basis for a jump test in Jiang and Oomen (2008).

of discretely sampled squared returns, and not just as a limiting result. Hence, it also provides exact valuation of variance swaps with payoffs determined by the cumulative sum of squared returns sampled at nontrivial intervals, such as daily.

These results carry over to traditional notions of return variation, if the approximation (6) is extremely close. Equation (5) suggests this may hold, but it is ultimately an empirical issue. Our analysis in Sections 3 and 4 is based on S&P 500 futures and covers an exceptionally volatile period, encompassing the crisis in 2008–2009, as well as the turmoil associated with the initial European sovereign debt crisis in 2010. As such, this sample contains extreme price movements and jumps, the exact features that may render the approximation poor. Thus, we compute the percentage deviation between the left- and right-hand sides of Equation (6). For June 2, 2008 – June 30, 2010, we construct realized volatilities, according to formulas (4) and (6), using 400 one-minute returns and "close-to-open" returns, capturing the volatility outside regular trading hours as well as over weekends and holidays. The median absolute deviation between RV^w and the weighted average of the usual measures, $\frac{2}{3}RV^c + \frac{1}{3}RV^s$, is a mere 0.0001% or 0.01 basis point, the mean deviation is 0.07 basis points (bps), and the maximum observed discrepancy is 0.0379% or less than 4 bps. Hence, the deviations are uniformly minuscule, economically negligible, and trivial relative to the (minor) market microstructure distortions we expect at these sampling frequencies for S&P 500 futures. Even during a regime with once-in-a-generation turbulence, the approximation is effectively perfect.

Having established theoretically, through a review of existing results, and empirically, through the virtual identity of the relevant realized volatility measures, that model-free implied volatility provides a valid valuation formula for the future return variation, even under price discontinuities and discrete sampling, we now move to novel refinements of the metric in the form of "corridor implied volatilities." Since this concept involves truncating the impact of large returns, the quality of the approximations only improve, and henceforth, we do not document this issue.

1.3 Corridor implied variance

In principle, the measurement of model-free implied volatility requires a continuum of strikes spanning the full support for possible futures prices, $(0, \infty)$. In practice, option quotes and prices are available only for a range around the forward (at-the-money strike) price. Thus, in practice, the measure is computed over a finite strike range only, and (inexpensive) far out-of-the-money (OTM) options are ignored. For example, the CBOE has a specific cutoff rule to determine which option quotes are used in computing the VIX. As we explain later, this truncation of the strike range can significantly impact the high-frequency properties of the implied volatility measure.

As a basis for analyzing truncated MFIV measures, we turn to the notion of corridor variance. For now, we fix the coverage $[B_L, B_H]$, $0 \leq B_L \leq B_H \leq \infty$. The associated corridor implied variance is

$$CIV = CIV(B_L, B_H) = 2\int_{B_L}^{B_H} \frac{M_0(K)}{K^2} dK. \tag{8}$$

In the case of a pure diffusive futures price and continuous trading, Carr and Madan (1998) show that CIV prices the expected return variation accruing within the corridor.[4] Below, we generalize this results to a setting with price jumps and discrete trading. It is of practical relevance as the computation of all existing VIX style indices exploits the type of truncation featured in the CIV formula (8).

Before stating the main corridor pricing result, it is convenient to introduce the following corridor truncation operator. For given B_L and B_H, let

$$\overline{F} = \begin{cases} B_L, & F < B_L \\ F, & B_L \leq F \leq B_H \\ B_H, & F > B_H. \end{cases} \tag{9}$$

Thus, $\overline{F}$ coincides with F within the corridor, but rounds to the nearest value of the corridor otherwise. With the help of (9), we define the corridor-truncated version of the squared weighted return as

$$\left(\bar{r}_i^w\right)^2 = 2\left(\frac{F_i}{\overline{F}_i}\left(\frac{\overline{F}_i - \overline{F}_{i-1}}{\overline{F}_{i-1}}\right) - \ln\frac{\overline{F}_i}{\overline{F}_{i-1}}\right). \tag{10}$$

It is easy to verify that, if F_{i-1} and F_i both are above or below the corridor, then the truncated return is zero. If F_{i-1} and F_i both reside within the corridor, then $\left(\bar{r}_i^w\right)^2 = \left(r_i^w\right)^2$. Hence, all price movements strictly within the corridor are included, while those occurring exclusively outside are excluded. However, more subtle issues arise when the price change involves crossing a corridor boundary. Our convention ensures exact valuation for the corridor return variation. Specifically, we have the following result when the corridor realized variance is defined as

$$CRV^w = CRV^w(B_L, B_H) \equiv \sum_{i=1}^{n} \left(\bar{r}_i^w\right)^2. \tag{11}$$

Proposition 2. For any partition $\mathcal{T}$, CIV reflects the fair valuation of CRV^w. That is,

$$E_0^{\mathbb{Q}}[CRV^w] = CIV = 2\int_{B_L}^{B_H} \frac{M_0(K)}{K^2} dK. \tag{12}$$

[4] Andersen and Bondarenko (2007) study several corridor implied volatility measures for the S&P 500. For example, the barriers $(0, F_0)$ and (F_0, ∞) generate down- and up-variance payoffs, respectively. Andersen and Bondarenko (2013) exploit such measures to shed light on the pricing of S&P 500 volatility risk on the upside versus downside.

Proof. See Appendix A.1. ■

Thus, the CIV formula—obtained by direct truncation of MFIV—prices the payoff defined through the cumulative contribution of the squared truncated returns $\left(\bar{r}_i^w\right)^2$. Moreover, as for the exact realized volatility valuation formula (7), the result applies for any discrete sampling scheme and arbitrary price jumps. Hence, the result generalizes the model-free valuation result in Bondarenko (2014) to the setting with corridor truncation.[5] Appendix A.2 establishes that the continuous-time limit for the corridor realized variance CRV^w is the corresponding corridor quadratic variation, denoted CQV^w.

2. Data

Our primary data source is tick-by-tick SPX option quotes from CBOE. The sample covers June 2, 2008 – June 30, 2010, encompassing 525 trading days. For the two nearby maturities, exceeding seven days to maturity, we have an average of about 213,000 (147,000) OTM put (call) option quotes per day.[6] We construct fifteen-second series for each of the available options across the active trading day, from 8:30 to 15:15 Central Time (CT), using the "previous tick" method.[7] If no quote arrives in an interval, the last available quote prior to the interval is used. In the case of inactivity, the quotes may be stale, so we impose a limit on the duration of widespread inactivity as described below. In addition, as a benchmark, we exploit the intraday quotes for the S&P 500 futures from the CME Group.

A few filters are applied to guard against data errors. First, we control for staleness by constructing our volatility indices using only recently updated quotes. Second, if larger blocks of adjacent OTM option prices are stale or missing due to a malfunction of the quote dissemination system, we eliminate the corresponding VIX observations to avoid "systemic staleness." Third, we impose a maximum threshold for the degree of no-arbitrage violations. Fourth, we use a bounceback filter to detect short-lived recording errors in the option quotes. It eliminates very few observations, but guards against errant outliers that induce multiple artificial jumps. We lose close to 1.2% of the fifteen-second observations due to our sequence of filters, with about half of the missing values stemming from the nonsystemic staleness requirement and half from the nonconvexity condition.[8]

[5] Bondarenko (2014) mentions the corridor application, but does not deliver any prescription for the suitable computation of the truncation returns. Likewise, the initial empirical work with corridor implied volatility in Andersen and Bondarenko (2007) fails to use the correct truncation returns for intervals in which the observed price crosses the corridor boundary.

[6] Thus, we have around 52(33.5) million OTM put (call) option quotes in the full sample. All trading days are included in the analysis, except for five holidays with limited trading hours.

[7] For each 15-second cross-section, we exploit an average of 66 (39) strikes for OTM put (call) options for the first maturity and 69 (43) strikes for OTM put (call) options at the second maturity.

[8] The procedures for implementing these filters are detailed in the Appendix C.

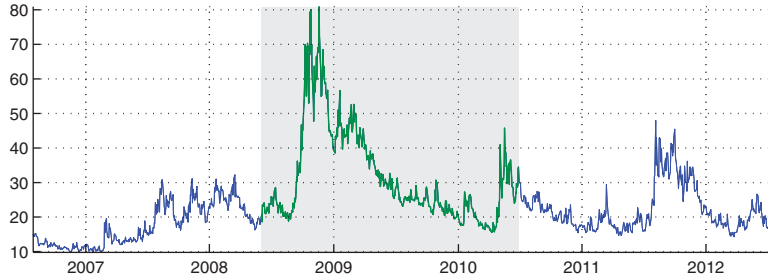

Figure 1
Daily closing value for VIX, January 2004 – August 2010
The units on the vertical axis are annualized percent. Our sample period, June 2, 2008 – June 30, 2010, is shaded.

The corresponding (official) fifteen-second VIX series is obtained from the real-time release by the CBOE. We apply a very mild filter to this series. We remove observations that fall outside the daily high-low range, as reported by CBOE at the end of trading. This merely reflects errors that have subsequently been recognized by the exchange. Second, we also apply the bounceback filter. We denote the resulting, lightly filtered series VIX*. Figure 1 shows the daily VIX closing value over recent years, with the shaded area indicating our sample period.

3. Construction and Properties of the Implied Volatility Indices

In this section we explore alternative high-frequency, model-free implied volatility series. We initially consider the CBOE VIX measure. Next, we exploit the comprehensive time-stamped SPX option quote data to generate a replication VIX index following the exact CBOE prescription. This enables us to assess various sources of noise in the officially disseminated series. The findings inspire the development of alternative model-free measures that provide a more suitable basis for studying the real-time equity-index volatility dynamics.

3.1 The VIX methodology

The CBOE volatility index, VIX, is explicitly designed to approximate the model-free implied volatility, or MFIV. The CBOE computes and disseminates the index value almost continuously during the trading day, effectively rendering the VIX observable in real time.

3.1.1 The actual VIX computation. The CBOE computes the VIX index from a set of European style OTM options written on the asset price with identical tenor, T, and strike prices K_j, $j=1,\cdots,N$, where $0<K_1<\cdots<K_f\leq F<K_{f+1}<\cdots<K_N$. Here, F represents the $t=0$ forward price of the asset for time T, and K_f denotes the first strike price available below the forward

price, where f is a positive integer, and a reasonable cross-section of options are available, so that $2 < f < N-1$.

The CBOE now computes the (annualized) model-free implied variance as follows

$$\widehat{\sigma}_T^2 = \underbrace{\frac{2e^{rT}}{T}\sum_{j=1}^{N}\frac{\Delta K_j}{K_j^2}M_0(K_j)}_{\text{Discrete Approximation}} - \underbrace{\frac{1}{T}\left[\frac{F}{K_f}-1\right]^2}_{\text{Correction Term}}, \tag{13}$$

where r denotes the (annualized) risk-free rate for $[0,T]$, proxied by the corresponding U.S. Treasury bill rate and $\Delta K_j = (K_{j+1} - K_{j-1})/2$.[9]

If we set r to zero (or value the options $M_0(K_j)$ in time T dollars), the first term of Equation (13) provides a direct discrete approximation to the theoretical MFIV in Equation (7), apart from the annualization factor $1/T$. The second term in Equation (13) adjusts for the lack of clean separation between the OTM put and call options, arising from the discrepancy between K_f and the forward price.

Another complication is that only a few option maturity dates are quoted at any given time, while VIX is defined for a fixed maturity of $T_M = \frac{30}{365}$, or thirty calendar days. The CBOE obtains the VIX measure by linearly combining $\widehat{\sigma}_1^2$ and $\widehat{\sigma}_2^2$ for the two expiration dates closest to thirty days with tenors of T_1 and T_2, but excluding options with less than seven calendar days to expiry. The interpolated quantity is expressed as a volatility measure and quoted in annualized percent,

$$VIX = 100 \times \sqrt{\left[w_1\left(\widehat{\sigma}_1^2 T_1\right) + w_2\left(\widehat{\sigma}_2^2 T_2\right)\right] \times \frac{365}{30}}, \tag{14}$$

where $w_1 = \frac{T_2 - T_M}{T_2 - T_1}$ and $w_2 = \frac{T_M - T_1}{T_2 - T_1}$, so we have $w_1 + w_2 = 1$.

The forward price F is not directly observable, so the exchange imputes it via put-call parity, using the pair of put and call options with identical strikes that has the smallest price discrepancy. Thus, all inputs for the VIX calculation, except for r, stem directly from the options data.

3.1.2 Tail truncation as a source of random bias in the VIX. Our objective is to obtain a high-frequency volatility series suitable for studying the dynamic features of equity-index returns. Any computational procedure will inevitably introduce some measurement and approximation errors into the index that may distort the properties of the series. For the VIX, Jiang and Tian (2005) identify a number of potential issues but conclude that, at the daily frequency, there

[9] At the boundaries, the CBOE defines $\Delta K_1 = K_2 - K_1$ and $\Delta K_N = K_N - K_{N-1}$, while $M(K_j)$ is the mid-quote for the OTM option with strike K_j. Specifically, $M_0(K_j)$ equals the put price when $K_j < K_f$, the call price when $K_j > K_f$, and the average of the two when $K_j = K_f$. See www.cboe.com/micro/vix/vixwhite.pdf for additional details.

are no major biases. In contrast, we find that idiosyncratic shifts in the strike range over which the $\widehat{\sigma}^2$ measure in Equation (13) is imputed have a systematic impact on key features of the high-frequency VIX index.

In principle, all (available) options should be exploited in computing the VIX index. In practice, however, the relative bid-ask spread is high for far OTM options and even midpoint quotes may be poor indicators of underlying value. Hence, the CBOE employs a specific cutoff rule: moving away from the forward price, once two consecutive strikes with zero bid quotes are encountered, all further OTM options are discarded. As documented below, this truncation produces a time-varying effective strike range, inducing noise and occasional spurious breaks, that is, artificial jumps, into the VIX series.

Therefore, conceptually, the VIX index is a corridor implied volatility measure subject to random truncation of the strike range. The variation measure in Equation (13) approximates the CIV measure,

$$\frac{1}{T} E_0^{\mathbb{Q}}[CIV] = \frac{2e^{rT}}{T} \int_{K_1}^{K_N} \frac{M_0(K)}{K^2} dK, \tag{15}$$

with barriers determined by the CBOE cutoff rule. The tail truncation implies that VIX^2 is downward biased relative to MFIV. If the truncation is subject to nontrivial idiosyncratic fluctuations, the VIX measure becomes incoherent: it does not capture an invariant notion of volatility. It reflects not only option prices (volatility) but also random shifts in the corridor. This implies that high-frequency VIX movements can be poor indicators of the actual volatility innovations, potentially rendering the VIX index unsuitable as an instrument for studying the dynamic interactions of returns and volatility.

The lack of precise indicators of value for deep OTM options is, of course, ubiquitous. It makes some kind of truncation or extrapolation inevitable in practice. We argue later that a useful solution is to ensure consistent truncation by adopting a coherent criterion for determining the strike range (K_1, K_N).

3.2 The VIX replication index, RX

As an initial benchmark, we construct a VIX "replication" series, RX, every 15 seconds, from the underlying SPX options in accordance with Equations (13) and (14), following the official CBOE procedure.[10] In principle, this series should mimic the VIX series disseminated by the exchange very closely, as they are extracted from the same set of underlying quotes across the trading day.

We have confirmed that the RX and VIX series evolve similarly, albeit not identically, in the vast majority of cases. However, importantly, we found

[10] We deviate slightly in our imputation of the forward price. The CBOE procedure lacks robustness to quote staleness and recording error. Hence, although we mimic the CBOE prescriptions in the vast majority of cases, we switch to a more robust computation when there are indications of a substantial bias. Our procedure is detailed in the Appendix B.

VIX to be lagged by 15–45 seconds relative to RX throughout the sample. Moreover, this lag fluctuates somewhat unpredictably over time. In short, the high-frequency VIX series, disseminated by the exchange, is not truly a real-time index.[11] Given our objective of matching the volatility series with the concurrent equity-index returns, this delay is troublesome. It implies we cannot accurately synchronize the VIX with other high-frequency series.

Since our RX index exploits time-stamped option quotes, it is immune to the computation and dissemination delays that affect the VIX series. As such, RX should be more timely and less error-prone than the official VIX release. For completeness, we report results based on both indices, while also checking that the evidence is consistent with our interpretations in this regard.

Another feature of concern is the presence of a surprisingly large number of abrupt moves in the high-frequency VIX series. While these may all represent valid discontinuities, or jumps, in the volatility process, they also can be due to purely idiosyncratic changes in the strike range. To control for the latter effect, we explore whether a given large 15-second move in the VIX is associated with a corresponding shift in the option prices, a sudden modification of the strike range, or both.

For this purpose, we define the effective range, or ER. For the strike range (K_1, K_N), it is given by,

$$ER = \left[\frac{\ln(K_1/F)}{\widehat{\sigma}_{BS}\sqrt{T}}, \frac{\ln(K_N/F)}{\widehat{\sigma}_{BS}\sqrt{T}} \right],$$

where $\widehat{\sigma}_{BS}$ denotes the at-the-money (ATM) Black-Scholes implied volatility (BSIV) measure.[12]

As an additional indicator, we also compute the VIX index using all OTM options with a positive bid quote. This corresponds to abandoning the cutoff rule based on two consecutive strikes with zero bid prices. Since the computation exploits the same or more options, the resulting index generally provides an upper bound for RX (and VIX). We denote this modified series RX*. Of course, whenever there are no options with a positive bid price beyond the CBOE truncation points, RX and RX* coincide.

Figure 2 illustrates why the strike range may be of concern. On February 16, 2010, our RX index replicates the VIX so well that they are indistinguishable at the granularity of the figure, and we only depict the former. It starts out, at 8:30, around 23.5, more than 2% below the RX* value of 24. The gap persists until about 11:00 when, in a matter of fifteen seconds, RX (and VIX) "jump." Subsequently, RX and RX* coincide and replicate the VIX closely. The explanation is evident from the bottom panel. The lower part of the strike

[11] This is likely due to capacity constraints of the CBOE server and in the associated dissemination system. This explanation arose from conversations with John Hiatt, Director of Research at CBOE.

[12] The implied volatility is obtained from a linear interpolation of four BSIV measures, extracted from options with strike prices just above and below the forward price for the two maturities closest to thirty calendar days.

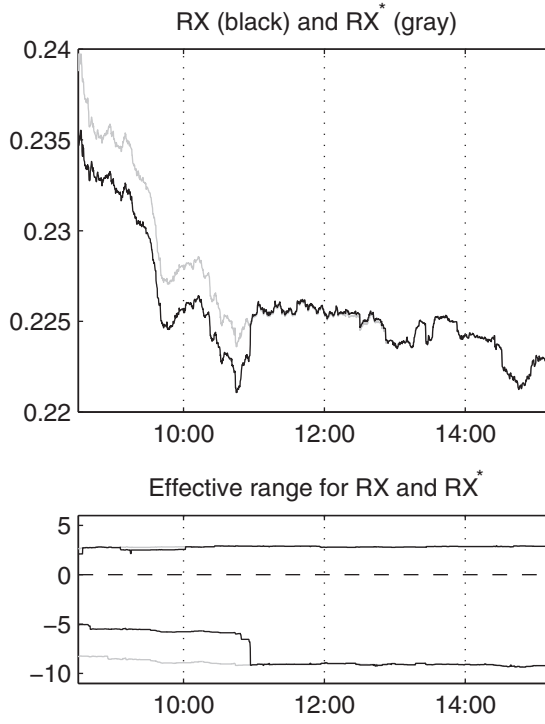

Figure 2
Volatility measures for February 16, 2010
The top panel depicts the RX and RX* volatility indices measured in annualized percentage, while the bottom panel displays the corresponding effective strike ranges measured in "sigmas" of Black-Scholes implied volatility.

range, representing OTM put options, expands suddenly at the time of the RX jump. In contrast, RX* is computed from a near-invariant range throughout. As such, the absence of a jump in RX* just before 11:00 indicates there is no meaningful shift in the option prices when the VIX jumps. The discontinuity arises solely from an abrupt expansion in the set of options used for the index computation.[13]

3.3 The corridor implied volatility index, CX

For corridor volatility to be useful, it must capture an economically invariant portion of the strike range across time. The following is desirable. First, the corridor is linked to observable option prices to facilitate real-time computation. Two, the forward price constitutes a natural focal point as it determines the OTM

[13] This type of artificial jump is not a rarity. Andersen, Bondarenko, and Gonzalez-Perez (2015) explore the quality of the high-frequency VIX series in detail and identify numerous similar incidents. Moreover, they find that RX* is subject to the phenomenon illustrated in Figure 2 as well.

options included in the computation. Third, the range adjusts endogenously to accommodate variation in the tails of the distribution. Fourth, the measure is model independent.

These considerations call for transparent and robust rules for determining the integration barriers of CIV in Equation (8). It turns out that the ratio of the put to the sum of the put and call option prices, at a given strike K, satisfies our criteria.[14] Formally, we define

$$R(K) = \frac{P(K)}{P(K)+C(K)}.$$

This ratio statistic depends only on option prices, so it is trivial to compute over the strike range for which we observe active quotes. Furthermore, $R(K)$ is akin to a cumulative density function (CDF) in that it is strictly increasing in K on $(0, \infty)$ with $R(0)=0$ and $R(\infty)=1$. In addition, the ATM put and call prices are theoretically identical, so $R(F)=0.50$, where the forward price F equals the mean of the risk-neutral distribution, that is, $F = E^{\mathbb{Q}}[F_T]$.

This has convenient implications. For a given percentile, $q \in (0, 1)$, we define the quotient $K_q = R^{-1}(q)$. It follows that if we use the percentiles of the ratio statistic, $R(K)$, to characterize the location of the strike K, the forward price constitutes the 50th percentile, or median, of $R(K)$,

$$K_{0.50} = R^{-1}(0.50) = F.$$

Consequently, the percentiles of the ratio function conveniently center the strike range on the focal point, F, for the computation of model-free implied volatility.

Figure 3 illustrates how option prices across a wide range of strikes are readily deduced from the available quotes. Only toward the tails of the distribution are option prices hard to measure accurately. The R function circumvents this issue, as it depends only on option prices within the selected strike range. If we define the corridor via symmetric percentiles of the R function, the truncation points will reflect the relative importance of the right and left tails for option pricing in a consistent manner. We settled on a 3% truncation level for the tails. This allows for a broad corridor, while ensuring that quotes spanning the width of the corridor are available for almost all high-frequency intervals across the sample.[15] The CX index is now computed exactly as the RX index, except that the barriers now are given by $B_L = K_{0.03}$ and $B_H = K_{0.97}$. The corresponding corridor variance measure follows from Equation (15):

$$CIV = \frac{2e^{rT}}{T} \int_{K_{0.03}}^{K_{0.97}} \frac{M(K)}{K^2} dK.$$

[14] These properties are also discussed in the concurrent work of Andersen and Bondarenko (2013).

[15] In Figure 3, we could readily expand the corridor without issues concerning reliable option quotes. Our more conservative cutoff guarantees there are quality quotes available across the predetermined corridor throughout the sample. Our results are robust to variation in the 3% threshold.

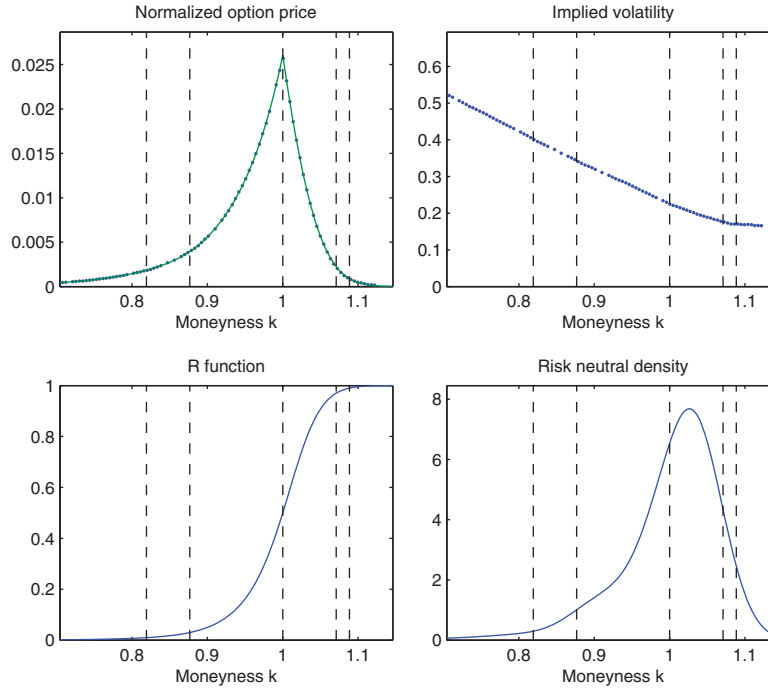

Figure 3
Determination of the CX truncation
The top left panel displays the normalized OTM option prices at the end of trading on June 16, 2010, for the thirty-day maturity. Moneyness is defined as $k = K/F$, while the normalized option prices are $\underline{M}(k) = M(k \cdot F)/F = M(K)/F$. The top right panel depicts the corresponding Black-Scholes implied volatilities, measured in annualized percentages. The bottom panels plot the extracted $R(k)$ function and estimated risk-neutral density. The vertical dashed lines indicate the 1th, 3rd, 50th, 97th, and 99th percentile quotients of $R(k)$.

3.4 Basic properties of the volatility indices

Existing option-based model-free implied volatility measures, including notably the VIX, are de facto corridor indices. As such, there are two primary differences between our CX index and measures computed according to CBOE prescriptions, like RX and VIX. First, CX explicitly controls the truncation to ensure the corridor width is computed consistently through time. Second, CX is based on a relatively narrow corridor to ensure that active option quotes are available for the relevant strike range across the full sample. Given the corridor construction, the CX index typically is lower than the corresponding RX and VIX values. This raises additional questions. First, do the indices differ in their characterization of the lower frequency evolution in volatility over time? Second, are there significant differences in the time-series properties at the high-frequency (return) level?

Table 1 provides summary statistics. To alleviate the effect of the dissemination delay in the VIX, they are compiled at the one-minute frequency. The left panel confirms that CX is lower than the other indices, both in

Table 1
Summary statistics for volatility indices

	Index level				Index return $\times 10^4$			
	CX	RX	VIX*	VIX	CX	RX	VIX*	VIX
Mean	29.03	31.58	31.71	31.72	−0.14	−0.11	−0.14	−0.15
SD	12.3	13.3	13.4	13.4	21.7	21.7	23.2	31.8
Skewness	1.32	1.33	1.32	1.32	0.33	0.11	−0.43	−0.71
Kurtosis	4.20	4.21	4.17	4.17	21.7	54.8	378	3758

This table provides summary statistics for the volatility indices CX, RX, VIX*, and VIX at a one-minute frequency. The statistics are reported for index levels, quoted in annualized percentage terms, and for their log returns.

terms of mean and standard deviation. In fact, both statistics are about 9% (8%) larger for VIX* (RX) than for CX, indicating that, to first order, CX is a down-scaled version of existing model-free implied volatility measures. This is corroborated by the scale-invariant skewness and kurtosis measures being remarkably similar, at around 1.3 and 4.2 across the board. Further, the correlations of CX with VIX* and RX exceed 99.9%. Thus, CX retains all key time-series properties of the VIX, but it is lower and thus does not approximate the (true) expected risk-neutral return variation. Rather, CX is deliberately scaled to ensure a consistent (corridor) notion of return variation over time.

In contrast, the high-frequency volatility increments display strongly divergent properties, as documented in the right panel of Table 1. The primary reason is that volatility innovations—in the absence of volatility jumps—scale with the time increment, while a shift in the set of options used for the index computation is independent of time scale. Thus, when the effective strike range changes, it has a dominant effect over a short time frame.[16] This has two major implications: (1) not only should the CX, on average, be lower than VIX style measures but also the relative value of CX versus VIX should be linked to the relative size of the underlying strike ranges, and (2) at high frequencies, VIX-type series will be noisier and, in particular, feature more outliers than CX. As a result, the skewness and kurtosis statistics for the volatility increments (returns) should differ markedly, providing a sharp contrast to the relation between these statistics for the index levels in the left panel of Table 1.

We explore the first implication through a simple regression, which also helps us to gauge whether variation in the range has an economically meaningful effect on the index values. Our dependent variable, $Z_t = RX_t/CX_t - 1$, equals the relative value of RX and CX at the end of trading on day t, while the explanatory variable, DR_t, represents the difference in the effective range for RX and CX.[17] We obtain the following regression result,

$$\begin{array}{rcccl} Z_t & = & 0.0340 & + & 0.0089\ DR_t, \qquad \bar{R}^2 = 67.2, \\ & & (6.76) & & (11.36) \end{array}$$

[16] This is analogous to the impact of microstructure noise on high-frequency-based realized volatility measures.

[17] The effective strike ranges for the two nearby maturities are constructed for each index and linearly interpolated to provide a thirty-day effective range. DR_t is then given by the difference between the ranges at this maturity.

where the t-statistics below the regression coefficients reflect Newey-West standard errors based on twenty lags. The discrepancy in the strike range has overwhelmingly significant explanatory power for the relative index values. The standard deviation of DR_t is 1.88, so, on average, an exogenous one-standard-deviation increase in the RX range inflates the value of RX relative to CX by an additional 1.7% (=1.88·0.89%). Thus, idiosyncratic variation in the strike range, unrelated to option prices and volatility, induces significant distortions in RX and, by extension, all other existing VIX-style indices.[18]

The evidence is also strongly supportive of the second implication, consistent with the presence of excessive idiosyncratic noise in the high-frequency VIX increments. While the sample kurtosis for the CX returns is sizeable, at around 22, the values for RX are imposing at around 55, and truly outsized for VIX. These discrepancies imply a much lower degree of cohesion between the index returns compared with their levels. The correlation of the CX and, respectively, VIX* and RX returns are 88.5% and 61.5%. Moreover, the fact that mild filtering reduces the kurtosis of VIX* dramatically compared with VIX implies that data errors contribute to the inflated statistics for the real-time VIX series. Our findings suggest there are important advantages in using CX in lieu of standard implied volatility measures for analyzing the high-frequency return dynamics. We turn to this task next.

4. The Dynamics of the Equity-Index Returns

The U.S. equity market undergoes intermittent periods of heightened volatility, often accompanied by bouts of sharply falling prices, while lower volatility usually coincides with an uneven ascent in prices. These features induce negative return skewness, see, for example, Harvey and Siddique (2000) and Albuquerque (2012). Nonetheless, we have only limited knowledge about the process by which the high-frequency return-volatility interaction propagates into the complex relation observed over lower frequencies.

In this section, we seek to enhance our understanding of the high-frequency return dynamics. From an empirical perspective, the main obstacle is the latent character of spot volatility. We circumvent this issue by exploiting our robust volatility series, CX. We first show that volatility jumps are common, nearly symmetric, and occur mostly when the underlying asset price also jumps. Next, we investigate the spot correlation between returns and volatility, documenting a very strong negative relation and a striking coherence between the estimates at different sampling frequencies. Finally, we illustrate how careful construction of the volatility index allows for improved real-time assessment of market

[18] A similar regression for the VIX* index produced almost identical results. In this case, we used the RX strike range as a proxy for the corresponding range for VIX*, whenever the two index values were close, while all other VIX* observations were excluded. Further details on the implementation and findings are available upon request.

conditions during periods when the trading process is operating under severe stress.

4.1 Volatility jumps

Standard asset pricing models almost invariably assert that spot volatility as well as the jump intensity and distribution in Equation (1) may be represented as smooth functions of a Markovian state vector, $\mathbf{S_t}$, which itself has a jump-diffusive representation.[19] Thus, we may write, for example, $v_t = v(\mathbf{S_t}, t)$. This implies that the state vector is critical also for the evolution of associated return variation measures. Specifically, as shown in Section 3, the implied volatility measures differ in their choice of corridor, but they all value the future return variation according to

$$\mathcal{V}_{t,T} = \frac{1}{T} E_t^{\mathbb{Q}}\left[CQV_{t,T}^{w}(B_L, B_H)\right], \tag{16}$$

where the corridor quadratic variance CQV^w is defined in (A.3). It then follows from standard assumptions, see for example, Todorov and Tauchen (2011), *Theorem 1*, that all the volatility indices also are smooth functions of the state vector. Thus, by Ito's formula for jump diffusions, there is a jump in the volatility index if and only if there is a jump in the underlying state vector and, by extension, a jump in the spot volatility. Moreover, standard models typically imply jump size monotonicity; that is, large jumps in spot volatility are associated with large jumps in implied volatility. Hence, (large) discontinuities in the high-frequency volatility index inform us about the jump activity in spot volatility and provide guidance regarding the jump size distribution as well.

4.1.1 Empirical evidence on volatility jumps. By far, the most common way to model jumps in volatility is through specifications allowing only for positive jumps. The reasons are threefold. First, positive volatility jumps are readily accommodated within the affine class of jump-diffusions, enabling tractable asset and derivatives pricing formulas. Second, the empirical distribution for volatility obtained from lower-frequency measures is right skewed, consistent with the presence of more upside than downside outliers. Third, from both risk management and asset pricing perspectives, positive volatility shocks are far more relevant for downside risk and risk premiums than for (potential) negative volatility jumps. Nonetheless, the development of suitable models–and the potential of acquiring a deeper understanding of the underlying mechanisms–requires a consensus regarding the basic features of the high-frequency return-volatility dynamics.

To alleviate distortions from microstructure noise, we again focus on one-minute changes, or returns, rather than on the original fifteen-second series.

[19] In fact, often, the spot volatility itself is assumed to be the sole state variable.

Table 2
Distribution of extreme returns ("jumps")

	CX	RX	VIX*	VIX
$(-\infty, -30)$	0	6	3	15
$(-30, -15)$	1	27	29	50
$(-15, -9)$	21	66	76	114
$(-9, -6)$	128	239	268	272
$(-6, -4)$	613	716	742	739
$(4, 6)$	590	725	730	731
$(6, 9)$	139	247	251	254
$(9, 15)$	10	79	93	131
$(15, 30)$	2	33	37	56
$(30, \infty)$	0	4	2	11

This table categorizes one-minute log returns of the volatility indices CX, RX, VIX*, and VIX, according to size in terms of "sigma," computed as specified in Appendix D.

In addition, liquidity is occasionally problematic at the market open, so we compute all statistics in this section for the 8:35-15:15 CT period only, excluding the initial five minutes of trading. Finally, while we focus on the results obtained via our CX series, we provide comparisons to findings based on alternative high-frequency VIX-style indices.

We proceed nonparametrically, defining large moves relative to a robust volatility measure, which accounts for time variation in volatility across days, as well as the pronounced intraday volatility pattern.[20] Exploiting this robust standard deviation measure, we sort the volatility returns into mutually exclusive size categories, measured in "sigmas." Table 2 tabulates the results.

The table reveals a startling discrepancy in the number of large moves across the indices, regardless of the threshold adopted for "identifying" jumps. For example, including moves beyond six standard deviations on the upside and downside, there are approximately 900 outliers in the regular VIX index and, respectively, 760 and 700 for VIX* and RX. In contrast, it is about 300 for CX. Hence, all indices display, on average, more than one large move every two trading days, and VIX tops the count with well in excess of one per day. The discrepancy in the number of moves beyond 15 "sigmas" is even more striking. The CX measure has three, whereas the count for the other indices is more than twentyfold higher. This is anomalous: any genuinely large shift in volatility should manifest itself in a significant elevation across a broad range of option prices and be reflected in any reliable implied volatility measure. Thus, our findings corroborate the hypothesis that measurement errors, including idiosyncratic fluctuations in the strike range, inflate the outlier count for many of the indices.[21]

[20] The procedure is detailed in Appendix D. The results are robust to alternative estimators of intraday volatility.

[21] The series underlying Table 2 consists of more than 200,000 one-minute returns, with the vast majority falling in the unreported $[-4, 4]$ standard deviation range. Since different filters are applied, the total number of observations for the indices differ slightly, but the results are unaffected by restricting the sample to a common set of one-minute returns.

Table 3
Binomial and Kolmogorov-Smirnov tests

		4	5	6	7	8	9	10	11	12
CX	Negative	763	326	150	82	38	22	8	5	3
	Positive	741	317	151	77	36	12	10	7	5
	p_{BN}	0.59	0.75	1.00	0.75	0.91	0.12	0.81	0.77	0.73
	p_{KS}	0.94	0.78	0.87	0.67	0.18	0.04	0.74	0.93	0.83
VIX*	Negative	1118	601	376	233	162	108	82	71	54
	Positive	1113	623	383	248	170	132	101	82	71
	p_{BN}	0.93	0.55	0.83	0.52	0.70	0.14	0.18	0.42	0.15
	p_{KS}	0.45	0.57	0.21	0.16	0.03	0.68	0.49	0.40	0.17

In each panel, the first two rows tabulate the number of one-minute log returns exceeding a specific (signed) threshold, while the last two rows provide p-values for the binomial (BN) and Kolmogorov-Smirnov (KS) tests for symmetry. The columns indicate the "jump" threshold in multiples of "sigma," computed as specified in Appendix D.

A second intriguing finding is the apparent symmetry of positive and negative "jumps" within each size category. A partial explanation is that misclassified jumps naturally revert, as an unusual narrowing of the strike range, say, often is followed later by a sudden reversal.[22] However, even for measures less prone to such errors, we observe an almost identical number of positive and negative jumps. Table 3 provides formal tests for (unconditional) symmetry of the jump distributions.[23] The results for CX confirm we cannot reject that the volatility jump distribution is symmetric. The evidence regarding VIX* jumps is similar, but it is less compelling, as many of these outliers are spurious.

Finally, we provide suggestive evidence regarding the time-series properties of volatility jumps. Figure 4 displays the CX returns exceeding six sigmas in absolute value across the full sample. The large volatility innovations are generally scattered widely across time, but there is a weak tendency for clustering, indicating potential time variation in the jump intensity. In addition, there is weak positive serial correlation in the direction of the jumps, although the large positive and negative volatility returns are quite evenly balanced over each three-month period in the sample. Notice also that the jump sizes are fairly homogeneous. Given that we measure the volatility increments in "sigmas," this implies that the (percentage) jumps tend to be larger when volatility is elevated. In other words, the volatility jumps are roughly proportional with the volatility level and therefore systematically larger during the financial crisis, say, than during more tranquil conditions.

4.1.2 Empirical evidence on the volatility-price jump interaction. We seek to characterize not only the nature of volatility jump, but also their

[22] Our bounceback filter mostly captures data errors that induce almost instantaneous corrections. Random variation in the width of the strike range typically persists and cannot be filtered without careful analysis of the underlying option data.

[23] The null hypothesis for the binomial test is that a given jump is positive with probability 0.5, so it checks whether the frequencies of negative and positive returns are statistically distinguishable. The Kolmogorov-Smirnov test checks whether the shapes of the empirical distribution for negative and positive returns are different, apart from the sign reversal.

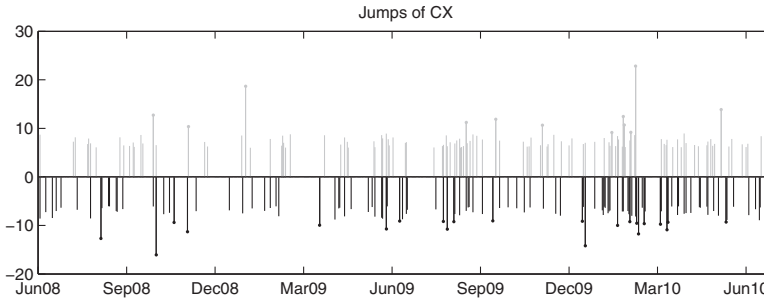

Figure 4
CX volatility jumps
This figure depicts one-minute log returns that exceed six "sigmas" in magnitude across the full sample. Sigmas are computed as specified in Appendix D. The returns exceeding nine sigmas have a circle at the end of their return bar. Positive (jump) return bars are gray, and negative return bars are black.

Table 4
The volatility jump distribution

	CX		SP		VIX*		SP	
	σ	%	σ	%	σ	%	σ	%
$(-\infty,-9)$	−10.47	−1.34	3.32	0.20	−14.31	−2.39	0.84	0.05
$(-9,-6)$	−7.02	−0.97	2.20	0.12	−7.10	−1.00	1.04	0.05
$(-6,0)$	−0.72	−0.13	0.49	0.04	−0.86	−0.14	0.48	0.04
$(0,6)$	0.70	0.13	−0.49	−0.04	0.85	0.14	−0.49	−0.04
$(6,9)$	7.08	1.04	−2.72	−0.17	7.06	1.09	−1.09	−0.07
$(9,\infty)$	12.81	2.34	−4.38	−0.40	13.70	2.24	−0.64	−0.04

This table categorizes one-minute log returns of the volatility indices CX and VIX*, according to size in terms of "sigma," computed as specified in Appendix D. For each category, the table reports the average jump size, measured in sigma and percent, along with the corresponding averages for the contemporaneous log returns of the S&P 500 futures.

interaction with the price dynamics and especially the incidence of price jumps. In this context, our findings raise several issues. First, can high-frequency price observations provide corroborating evidence for the presence of negative volatility jumps? Second, do the concurrent returns display similar qualitative features in the event of positive and negative volatility jumps? Third, is there evidence of return-volatility cojumps? Fourth, the results for our corridor index, CX, should differ systematically from those obtained via the VIX* series if the latter contains artificial jumps. Is this prediction confirmed?

Consequently, we now provide a comprehensive analysis of the relation between innovations in the volatility indices and the contemporaneous asset returns. Table 4 reports the average volatility and equity returns in "sigmas" and percentages across six size categories for the volatility innovation. Informally, we classify (absolute) changes of more than six sigmas as jumps, with the ranges (-9,-6) and (6,9) corresponding to large jumps and those exceeding nine sigmas (in absolute terms) indicating extreme jumps. The left panel reveals a strong inverse monotonic relationship. For all size categories, positive CX innovations

are associated with negative equity returns and negative CX moves with positive returns. Thus, the pronounced negative association between volatility and return innovations is in force, not just for small CX returns but also for extreme innovations, reflecting volatility jump realizations.

The right part of Table 4 provides the corresponding average innovations for the VIX* and S&P 500 series, sorted according to the size of the VIX* increments. While the qualitative features are similar to those in the left panel, the negative association is substantially weaker. For every category, the S&P return innovations are smaller than for the corresponding CX grouping, and the monotonic relation between the sizes of the volatility and return innovations has been lost, as the (absolute) equity returns are higher for medium than extreme volatility increments. This is consistent with the VIX* series being contaminated by large "artificial" jumps induced by idiosyncratic shifts in the strike range.

Given the neglect of negative volatility jumps in the literature, the evidence is startling. There is no visible difference between the positive and negative CX jumps. They appear symmetric and share a distinct negative association with the underlying returns process across all size categories. Moreover, the findings for VIX* are consistent with these conclusions, as the VIX* correlation with the returns is downward biased due to the additional noise in this series. To further explore the robustness of these results, we now focus on the entire distribution of the equity returns conditional on a jump in volatility.

The right top panel of Figure 5 displays smoothed density estimates for the S&P 500 returns conditional on the CX increment falling within, respectively, the intervals of (-9,-6) or (6,9) sigmas, while the left panel provides the corresponding scatter plot for the volatility and equity returns along with the (negatively sloped) regression line. The densities are symmetric and nearly identical apart from a shift in location. The returns corresponding to negative volatility jumps are drawn from a distribution with a large positive mean and a nontrivial variance, while those associated with positive volatility jumps are drawn from a similar distribution, except the mean is now large and negative. Hence, yet again, the negative volatility jumps are qualitatively related to the asset returns in the same manner as the positive volatility jumps. We conclude that there is a genuine pronounced negative and monotone association between the return and volatility innovations, regardless of sign and size. For completeness, the corresponding VIX* displays are provided in the bottom panels of Figure 5. The numerous observations scattered along the extreme left and right ends of horizontal axis are consistent with the presence of artificial jumps. In these instances, the VIX* index changes abruptly, but options prices barely move, indicating a sudden shift in the strike range, as exemplified in Figure 2. The additional noise in VIX* also manifests itself in the distinctly less negatively sloped regression line in the lower left panel.

Figure 5 suggests a cojumping relationship between the equity-index returns and CX and, by extension, between returns and spot volatility. To shed

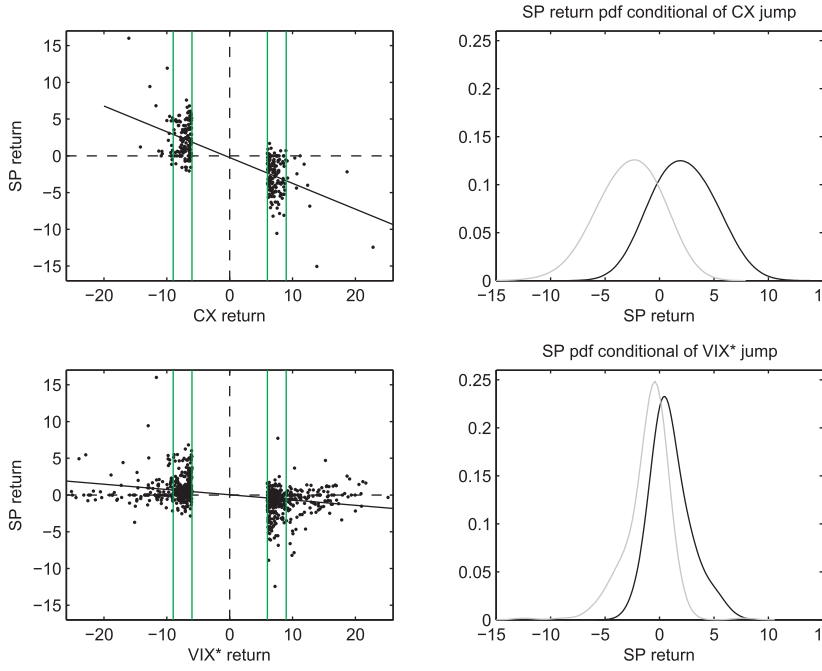

Figure 5
S&P 500 versus jumps in CX and VIX*
The top left panel is a scatter plot of one-minute log returns of the S&P 500 futures versus returns of CX. Returns are expressed in "sigma," computed as specified in Appendix D. Returns are only shown when the absolute return of CX is greater than six sigmas. The top right panel is a probability density of S&P 500 constructed using kernel smoothing for two cases, when CX return is between $(-9,-6)$ (black) or between $(6,9)$ (gray). The two cases are also indicated by vertical lines on the left panel. The two bottom panels repeat the same exercises, but now for VIX* instead of CX.

Table 5
Jumps in S&P 500 and volatility indexes

	SP		CX		VIX^*	
	σ	%	σ	%	σ	%
$(-\infty,-6)$	−7.45	−0.54	6.54	1.49	4.12	0.90
$(-6,-4)$	−4.57	−0.26	3.70	0.63	2.68	0.43
$(-4,0)$	−0.89	−0.06	0.56	0.11	0.44	0.08
$(0,4)$	0.89	0.06	−0.59	−0.12	−0.46	−0.08
$(4,6)$	4.61	0.28	−3.61	−0.59	−2.90	−0.46
$(6,\infty)$	7.58	0.59	−6.32	−1.13	−3.19	−0.39

This table categorizes one-minute log returns of the S&P 500 futures, according to size in terms of "sigma," computed as specified in Appendix D. For each category, the table reports the average return size, measured in sigma and percent, for S&P 500 and the volatility indexes CX and VIX*.

additional light on this relation, we reverse the perspective and explore the distribution of the volatility increments conditional on a large return innovation. In Table 5, we sort the observations according to the size of the one-minute S&P 500 return and report the mean values for the volatility index and return

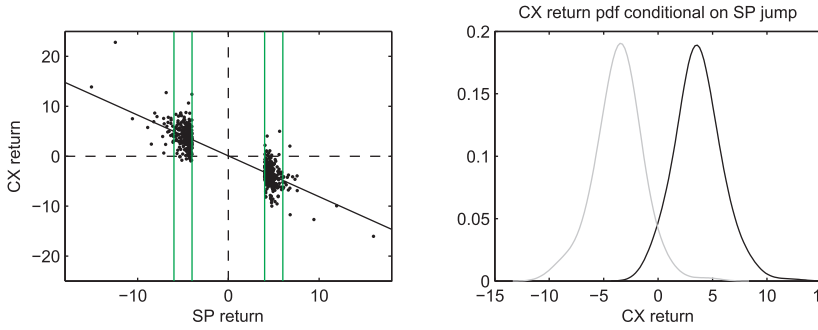

Figure 6
CX and jumps in S&P 500 futures
The left panel is a scatter plot of one-minute log returns of CX versus returns of S&P 500 futures. Returns are expressed in "sigma," computed as specified in Appendix D. Returns are only shown when the absolute return of S&P 500 exceeds four sigmas. The right panel is a probability density of CX constructed using kernel smoothing for two cases, when the S&P 500 return is between $(-6,-4)$ (black) or between $(4,6)$ (gray). The two cases are also indicated by vertical lines on the left panel.

innovations within each group. Consistent with our prior findings, a pronounced negative association between the CX and equity-index returns is apparent, while the relation between the VIX* and S&P 500 returns is weaker. The right panel of Figure 6 displays the smoothed empirical density for the CX returns conditional on the S&P returns falling within the intervals of $(-6,-4)$ or (4,6) sigmas. The figure confirms the stark negative association between the return and volatility innovations and a near-perfect mirror-image symmetry for the volatility increments corresponding to negative and positive equity returns.[24] Overall, the evidence is strongly supports of a contemporaneous inverse cojumping relation between volatility and returns.

In summary, our evidence paints a starkly different picture relative to the extant asset pricing literature. We identify more volatility jumps than have prior studies. For example, Broadie, Chernov, and Johannes (2007) stress that jumps are rare–1-2 annually–so 15-20 years of data is insufficient for inference.[25] In contrast, we identify the same number of jumps in about a month! Discontinuities are, almost tautologically, more readily identified from high-frequency data, implying that a finer "microscope" is needed for a thorough exploration of the interaction between volatility and price jumps. Moreover, the symmetric jump distribution is at odds with the presumption that volatility only jumps upward. Most importantly, it violates the basic structure of the tractable class of affine jump-diffusive models.[26] The finding also has implications for the source of skewness in lower frequency equity returns. If the joint return and

[24] As expected, the comparable figure for the density of VIX* returns conditional on large innovations in the equity-index returns display a qualitatively similar, albeit weaker, relationship.

[25] See their paper for numerous studies reaching similar conclusions from daily data.

[26] See Amengual and Xiu (2014) for a recent study exploring negative volatility jumps with daily data.

volatility distribution is symmetric, that is, large positive return and negative volatility jumps are as prevalent as negative return and positive volatility jumps, then the skewness in the marginal return distribution does not originate from more frequent and large negative price jumps or more frequent and large positive volatility jumps. Instead, the lower frequency return skewness is a dynamic phenomenon, generated by the increased volatility accompanying price drops. This feature increases the probability that large negative shocks are followed by additional large shocks (of either sign), while large positive returns in contrast dampen the turbulence. Hence, volatility is sustainable only if the market is hit by a sequence of large negative shocks, which, in turn, is more likely if volatility is already elevated.

4.2 Asymmetries in the return-volatility relation

The asymmetric relation between equity return and volatility innovations is known as the "leverage effect," following Black (1976) and Christie (1982), who stressed the increased financial leverage, and thus higher return volatility, induced by declining equity prices. The "leverage" label has stuck although, subsequently, the impact of financial leverage has been found to be quantitatively much too small to rationalize the strong negative association in the data, see, that is, Duffee (1995) and Bekaert and Wu (2000). An alternative reverse causality is often invoked: an increase in market volatility commands an increased equity risk premium, inducing a concurrent drop in equity prices, see, for example, French, Schwert, and Stambaugh (1987) and Campbell and Hentschel (1992). Recognizing these features, Nelson (1991), Engle and Ng (1993), and Glosten, Jagannathan, and Runkle (1993) incorporate correlations between return and volatility innovations into GARCH models, estimated from daily asset returns. However, an accurate quantification requires observations at a much higher frequency. Moreover, we aim to develop tools for measuring the effect over relatively short intervals so that we can explore whether the correlation structure varies in conjunction with market conditions.

Our evidence in Section 4.1 is consistent with a pronounced leverage effect. Tables 4 and 5 suggest a strong asymmetric relation between regularly sized (non-jump) price and volatility moves as well as for cojumps. The pertinent question is whether the negative association is similar across diffusive moves and jumps. The literature estimating the effect from high-frequency data has restricted attention to the correlation of diffusive return and volatility innovations within a specific setting, for example, the one-factor Heston model, or an asymptotic correlation measure that excludes jumps.[27]

We view the leverage coefficient as a measure of the overall contemporaneous return-volatility relation, not just the diffusive interaction, so we define it via

[27] See, for example, Aït-Sahalia, Fan, and Li (2013) for implementations along these lines.

the limiting return-spot volatility correlation,

$$\mathscr{L}_t = \lim_{\Delta \to 0} Corr(s_t - s_{t-\Delta}, v_t - v_{t-\Delta}), \tag{17}$$

which, in general, depends not only on the diffusive leverage but also on the (conditional) jump intensities and expected jump sizes for idiosyncratic price and volatility jumps as well as cojumps.

It is infeasible to procure reliable empirical estimates for the local leverage measure, as stated in Equation (17) without imposing strong identifying assumptions. We initially discuss a restrictive framework in which consistent estimation is possible and then argue, based on extensive empirical robustness checks, that the overall estimates are remarkably stable to shifts in the estimation design.

4.2.1 Estimating the leverage coefficient in one-factor diffusive models. Within a continuous time setting, the leverage effect largely has been estimated via one-factor diffusive representations. In this section, we follow this setup and assume the return dynamics is given by

$$\frac{dF_t}{F_t} = \mu_t dt + \sqrt{v_t} dW_t,$$

where the state vector simply equals spot volatility, that is, $\mathbf{S_t} = v_t$. The key complication in estimating the leverage coefficient is the lack of a directly observable series for spot volatility. We circumvent this problem by exploiting a model-free measure in lieu of spot volatility. As noted in Equation (16), the former is related to the latter through a smooth-monotone mapping. Under standard assumptions, the implied volatility measures are now also governed by a one-factor diffusion (under $\mathbb{Q}$) of the form

$$d\mathscr{V}_{t,T} = \xi(v_t)dt + \sqrt{\psi(v_t)}dB_t \qquad \text{and} \qquad Cov(dW_t, dB_t) = \rho_t dt, \tag{18}$$

with $\xi(\cdot)$ and $\psi(\cdot)$ being smooth functions of spot variance.

For this class of models, we may recover the leverage effect directly from the (instantaneous) correlation of the observable price and volatility index innovations. This follows directly, by Ito's Lemma,[28]

$$\mathscr{L}_t = \frac{Cov(dF_t/F_t, d\mathscr{V}_{t,T})}{\sqrt{Var(dF_t/F_t) \cdot Var(d\mathscr{V}_{t,T})}} = \frac{\sqrt{v_t}\sqrt{\psi(v_t)}\,\rho_t}{\sqrt{v_t \cdot \psi(v_t)}} = \rho_t. \tag{19}$$

[28] The result accommodates all standard one-factor models involving dynamic specifications for the square root or logarithm of v_t. For example, Bandi and Reno (2012) explore the log-volatility specification. Wang and Mykland (2014) also stress the invariance of the leverage coefficient to the functional form linking the spot volatility and the state vector.

4.2.2 The basic estimator for the leverage coefficient. The upshot of the prior section is that, subject to the one-factor diffusive assumption, the leverage coefficient can be identified from the high-frequency correlation between returns and volatility indices in a model-free fashion. Unfortunately, the one-factor specification is restrictive. Empirical studies invariably conclude that diffusive models should contain at least two volatility factors. In addition, as demonstrated in Section 4.1, the evidence for jumps, and cojumps, in price and volatility is compelling. Such features complicate the task of designing suitable local measures of leverage. For example, if jumps are rare, then the empirical correlation obtained over short time intervals will not capture the average, or expected, impact of the jump activity. One response is to restrict attention to the diffusive return-volatility correlation and annihilate the impact of large (jump) innovations. Likewise, if there are multiple factors, the return-implied volatility correlation will not consistently estimate the leverage effect, as the separate dynamics of the volatility factors will induce a maturity effect, that is, the correlation will in general depend on the tenor of the options used to construct the index.

Given these complications, we proceed sequentially. In this section, we estimate the leverage coefficient using the natural framework under the one-factor diffusive assumption. In the subsequent section, we explore the sensitivity of the findings to variation in the estimation procedure, designed to detect a potential lack of robustness induced by the presence of jumps or multiple volatility factors.

Our basic estimator is designed to accommodate potential time variation in the leverage coefficient. We follow Kalnina and Xiu (2014) in defining the integrated leverage over the interval $[t, t+\tau]$ as[29]

$$I\mathscr{L}_{t,\tau} = \frac{1}{\tau} \int_t^{t+\tau} \mathscr{L}_u \, du, \tag{20}$$

which represents the time-averaged spot leverage over the interval. This differs from the ratio of the covariance over the product of standard deviations measured across the full period, if the second return moments are time varying. The spot estimate at time t may be obtained from the correlation of high-frequency return and volatility increments in a local neighborhood of t.[30] To obtain the overall integrated leverage, we simply average the individual spot leverage estimates over the relevant sample.

[29] Kalnina and Xiu (2014) was conceived independently but appeared after the original version of our paper. They focus exclusively on estimation of the leverage effect and the associated asymptotic theory, exploiting the general framework of Jacod and Rosenbaum (2013), so they complement our analysis. In the empirical work, they do not utilize the notion of corridor volatility and reach somewhat different conclusions. This may stem from the use of less robust volatility measures.

[30] The estimator relies on an asymptotic scheme letting the high-frequency innovations be sampled ever more finely as the local neighborhood shrinks; we refer to Kalnina and Xiu (2014) for details.

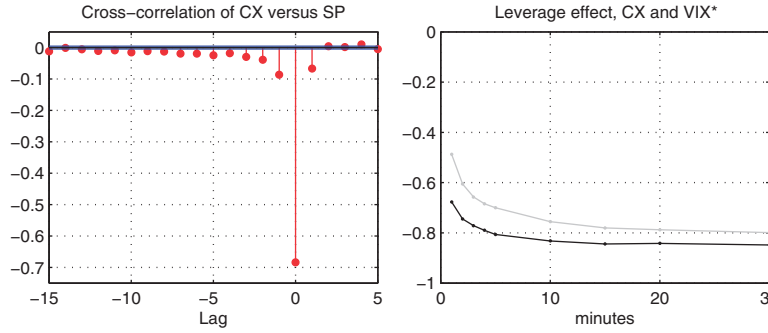

Figure 7
Cross-correlation and signature plot
The left panel depicts cross-correlations of CX versus S&P 500 futures. The right panel depicts the correlations of CX (black) and VIX* (gray) with the S&P 500 futures across frequencies.

In practice, market microstructure frictions limit the sampling frequency advisable for estimating variances and, especially, covariances. Up to this point, we have used one-minute increments, motivated by the absence of significant serial correlation in the corresponding returns. However, the negative higher order cross-correlations in the left panel of Figure 7 are indicative of potential staleness in the volatility indices. This implies that correlation measures constructed from one-minute returns may be biased toward zero, a situation referres to as the so-called Epps effect. To explore the severity of this feature, we construct a "signature leverage plot," displaying integrated leverage as a function of the underlying sampling frequency. In all cases, the local neighborhood is one trading day, so each point in the right panel of Figure 7 represents the sample average of the daily leverage estimates obtained at this frequency.

The signature plot confirms the presence of a significant Epps effect. The integrated leverage declines systematically as the sampling frequency goes beyond ten minutes but is stable at a value below -0.80 for lower frequencies. Motivated by these findings, we employ ten-minute returns for estimating of the leverage effect below. Finally, the estimates obtained from CX are lower than those associated with VIX*. This is consistent with a bias generated by noise in the VIX* series, stemming from idiosyncratic variation in the strike range and random delays in the quote dissemination.

Our estimate of an (integrated) leverage coefficient below -0.80 is remarkable given the substantially less negative estimates obtained in prior studies. Next, we explore the robustness of our result.

4.2.3 Alternative estimates of the leverage coefficient. The estimates in Figure 7 contain no corrections for jumps or cojumps. A simple robustness

Table 6
Correlation of volatility indices with S&P 500 returns

	Futures			Futures, bias-corrected			Forward		
	CX	RX	VIX*	CX	RX	VIX*	CX	RX	VIX*
$(0,3)$	−0.814	−0.788	−0.762	−0.817	−0.791	−0.766	−0.835	−0.808	−0.774
$(0,4)$	−0.826	−0.799	−0.774	−0.829	−0.803	−0.777	−0.844	−0.815	−0.784
$(0,6)$	−0.830	−0.803	−0.777	−0.833	−0.806	−0.780	−0.846	−0.816	−0.787
$(0,9)$	−0.832	−0.795	−0.771	−0.835	−0.799	−0.775	−0.848	−0.808	−0.783
$(0,\infty)$	−0.832	−0.781	−0.756	−0.835	−0.784	−0.759	−0.848	−0.793	−0.768

The correlations are reported for CX, RX, and VIX* with respect to S&P 500 futures (left panel), S&P 500 futures and biased-corrected following the procedure of Kalnina & Xiu (2014) (middle panel), and S&P 500 forward price implied by put-call parity (right panel). The correlations are obtained from ten-minute log returns. The first column indicates the set of volatility innovations used to compute the correlations. The innovations are expressed in "sigma," computed as specified in Appendix D.

check is to exclude the largest innovations, presumably signifying jumps.[31] Specifically, we investigate the sensitivity of the leverage estimate to the elimination of outliers of varying size. We summarize the findings in Table 6. We observe a striking consistency regardless of whether all large volatility innovations are excluded, all are retained, or an intermediate cutoff level is applied. Invariably, the integrated leverage for the full sample, estimated from CX and futures returns, falls between -0.81 and -0.84. We observe a similar degree of stability for the alternate volatility series in most cases, even if they are slightly closer to zero. The exception is the category including the most extreme jumps, where the estimates shrink more significantly. Again, these discrepancies are consistent with the presence of "artificial" jumps in the VIX indices. Finally, we note that the conclusions are largely unchanged if we implement a formal bias correction procedure, proposed by Kalnina and Xiu (2014), as shown in the middle panel, or rely on the correlation between CX and implied forward rate innovations, as displayed in the right panel.

The invariance of leverage to jumps is tantalizing. It suggests the interdependencies between the return and volatility innovations in the diffusive and jump components are similar. This has ramifications for the specification of asset pricing models, which usually accommodate neither the symmetric (marginal) jump distribution for return and volatility nor their strongly negative cojump relation.

A second concern is the potential divergence between the correlation of returns with spot volatility versus (longer maturity) implied volatility. In multifactor settings, the diffusive coefficients governing the dynamics of implied volatility are generally functions of option tenor. Hence, if this constitutes a problem, we should expect to find a systematic maturity effect in the estimates. Thus, we now explore whether our leverage estimates are sensitive to the underlying option tenor.

[31] Formal asymptotic justification for this type of procedure is provided by Kalnina and Xiu (2014).

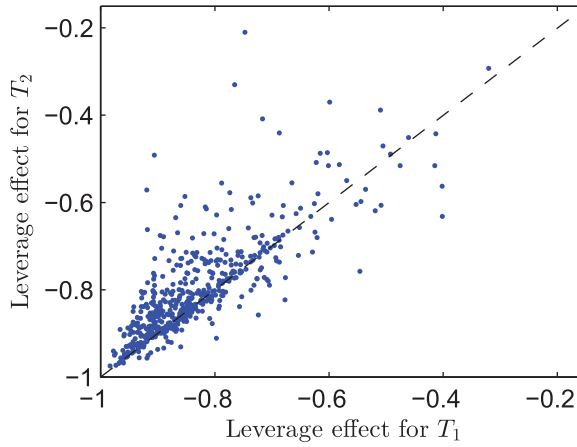

Figure 8
Scatter plot of leverage effect for two maturities
T_1 and T_2 are the option first and second maturities. The leverage effect is computed with respect to the S&P 500 futures using ten-minute log returns.

The CX index is computed from options across two separate maturities. Figure 8 plots the leverage coefficients obtained if we use only the shorter, respectively, longer, maturity options in the computation. The figure documents overall good coherence between the results from each of the constituent CX indices, with both maturities implying an unconditional leverage effect of roughly the same magnitude and substantially lower (more negative) than existing estimates in the literature. Nonetheless, there is a tendency for the estimates to be a bit larger (less negative) for the shorter maturity. Absent measurement issues, we prefer the maturity to be as short as possible. However, short-dated OTM options are inexpensive, implying larger percentage bid-ask spreads and fewer option quotes included in the CX computation. The first feature induces a larger relative measurement error for each individual option, and the second implies less error diversification from the aggregation of the options across the strike range. Consequently, the short maturity CX measures are exposed to a larger degree of noise, thus biases the empirical correlation measures toward zero. These considerations imply a trade-off between maturity and relative precision. As we move from very short tenors toward more intermediate values, the noise should decline and the leverage estimates increase, but eventually the relative pricing errors are sufficiently small that the maturity effect becomes the dominant concern.

To more systematically explore whether such maturity effects are operative, we now focus on CX measures based on options with tenor ranging from quite short (7–21 calendar days), through a couple of intermediate groups (22–35 and 36–49 days), to fairly long (over 50 days). The categories are constructed to ensure a reasonably uniform maturity within each group, while allowing for

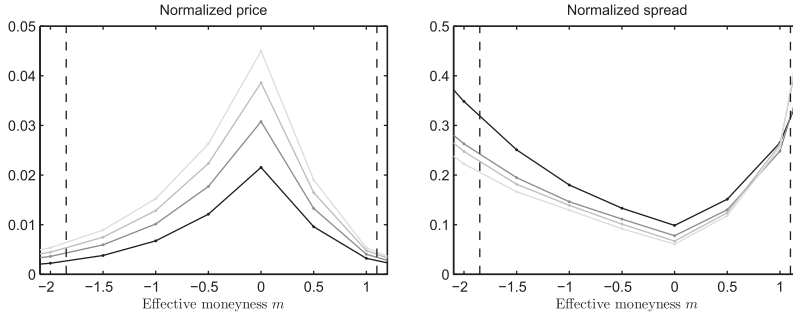

Figure 9
Liquidity measures for S&P 500 options
The normalized option price and normalized bid-ask spread are plotted for different levels of effective moneyness $m = \frac{\ln(K/F)}{\widehat{\sigma}_{BS}\sqrt{T}}$. The normalized price is M/F, where $M = \frac{1}{2}(A+B)$ and A and B are the dollar ask and bid prices; the normalized spread is $(A-B)/M$. The measures are computed separately for maturity categories $C_1 - C_4$ (from black to light gray) with 7–21, 22–35, 36–49, and 50+ days, respectively. For $m<0$, puts are used; for $m>0$, calls are used; and for $m=0$, the average of puts and calls is used. The dashed vertical lines indicate the average effective range of CX.

Table 7
Leverage effect for different maturities

	T_M	T_1	T_2	C_1	C_2	C_3	C_4
Mean	−0.832	−0.801	−0.836	−0.791	−0.816	−0.838	−0.829
SD	0.104	0.114	0.105	0.123	0.099	0.103	0.111
5%	−0.950	−0.941	−0.951	−0.940	−0.943	−0.948	−0.952
25%	−0.905	−0.879	−0.909	−0.875	−0.883	−0.909	−0.904
50%	−0.856	−0.830	−0.860	−0.823	−0.838	−0.863	−0.853
75%	−0.790	−0.744	−0.795	−0.736	−0.763	−0.798	−0.791
95%	−0.623	−0.579	−0.622	−0.555	−0.643	−0.608	−0.611

This table reports summary statistics for the leverage effect for different maturities, where T_M is constant maturity (one month), T_1-T_2 are the option first and second maturities, C_1-C_4 represent maturity categories with 7–21, 22–35, 36–49, and over fifty calendar days. The correlations are computed with respect to the S&P 500 futures using ten-minute log returns.

a comparable number of options across categories. The left panel of Figure 9 depicts the relative pricing of the options. As conjectured, more options are included in the CX computation for the longer maturities, with the average number of strikes used being, respectively, 30, 42, 52, and 57. Moreover, the short maturity options have a wider percentage bid-ask spread. The normalized (relative) spread is depicted in the right panel of Figure 9. This effect, combined with the lower degree of error diversification, induces additional noise into the corridor volatility computation at shorter maturities.

Table 7 provides further details regarding the distribution of the estimated leverage coefficients across maturities. Evidently, the shortest maturity CX indices (T_1 and C_1) are associated with more volatile estimates, while the most stable estimates are obtained from the intermediate tenors (C_2 and C_3). Moreover, there is a close correspondence between the distribution of estimates

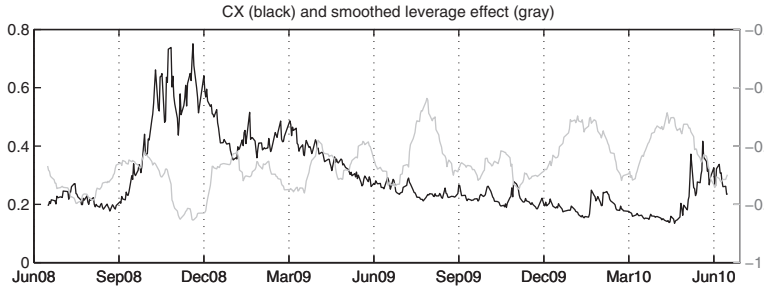

Figure 10
CX and leverage
CX is black, and the leverage coefficient is gray. The leverage effect is computed with respect to the S&P 500 futures using ten-minute log returns and is averaged over a moving centered window of 21 days.

for the fixed monthly horizon, T_M, and those for the intermediate tenors, C_2 and C_3.

In summary, the mean and median values for integrated leverage of -0.83 and -0.85 based on the CX measure with a fixed monthly tenor, T_M, are robust to the exclusion of large return and volatility jumps as well as reasonable variation in the underlying option maturities. Our highly negative estimate marks a substantial departure from the extant literature. For example, Bandi and Reno (2012) find the coefficient mostly ranging from –0.22 to –0.35 and only reaching –0.45 for exceptional levels of realized volatility. Ishida, McAleer, and Oya (2011) exploit high-frequency VIX data directly and obtain alternative GMM based estimates spanning –0.51 to –0.57. Finally, exploiting the strict assumptions of the one-factor Heston model, Aït-Sahalia, Fan, and Li (2013) arrive at a point estimate of –0.676. Our estimate based on the high-frequency CX series also surpasses the large negative value obtained by the CBOE from daily VIX and equity returns over the corresponding sample period.

4.2.4 Time-variation in the leverage coefficient. Figure 8 and Table 7 suggest the leverage effect may vary across the sample. Figure 10 plots the centered 21-day moving average of the integrated leverage estimates against the concurrent CX index. First, we note that the monthly leverage coefficients fall between -0.67 and -0.92. Even the highest (least negative) of these estimates are below the ones obtained in most published studies. Second, there are cyclical patterns in the series, with leverage increasing as CX declines. This is most evident in the sharp decline during the September-December 2008 crisis, where it reaches the most negative level over the sample, and then the substantially higher levels attained as volatility reverts back toward more normal levels from mid-2009 until early 2010. Finally, the leverage again reaches extreme negative values as volatility spikes during the European sovereign debt crisis in the spring and summer of 2010. The countercyclical movement in leverage is also apparent from the scatter plot in Figure 11. To the extent that high CX

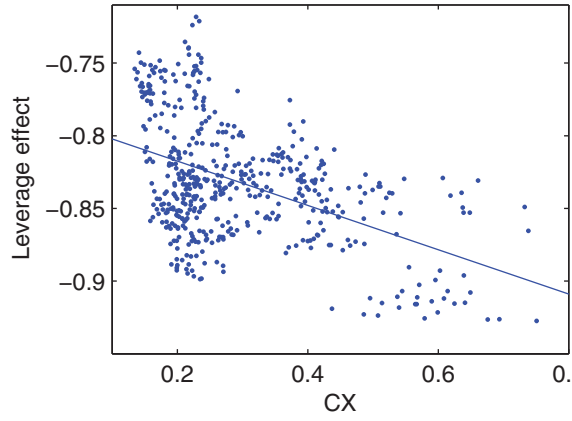

Figure 11
Scatter plot of leverage versus CX
The leverage coefficient is computed with respect to the S&P 500 futures using 10-minute log returns and it is averaged over a moving centered window of 21 days.

values proxy for market turbulence and economic uncertainty, the leverage grows sharply stronger (more negative) during downturns. Even if the sample is short, preventing us from drawing firm conclusions, the finding is intriguing. Periods with high implied volatility have been found to involve an unusually large variance risk premium and an elevated equity risk premium. Hence, the increasing (absolute) leverage coefficient during such periods suggests that the effect is associated with risk pricing.[32]

We emphasize that the ability to measure the leverage coefficient fairly accurately at a high frequency is key to our analysis. This is, seemingly, infeasible with a methodology relying exclusively on equity-index returns.[33] As such, our methodology opens up new avenues for empirical and theoretical work regarding the equity index return-volatility asymmetry.

4.3 Volatility indices during periods of market stress: The flash crash

On May 6, 2010, just after 13:30 CT, the S&P 500 index dived by more than 5% in a matter of minutes, only to rapidly recover thereafter. Most other U.S. securities markets underwent corresponding whipsawing trading patterns, pointing toward a breakdown in cross-market liquidity. This decline and rebound was unprecedented in speed and scope. The event is now known as

[32] See, for example, Nagel (2012) for a broader discussion of the evidence relating implied volatility and risk premiums.

[33] Bandi and Reno (2012) also find evidence for an increasingly strong leverage effect during high volatility periods, but their average estimates are much less pronounced. However, for return-volatility cojumps, Bandi and Reno (2015) report estimates at the other extreme, namely, very close to -1.

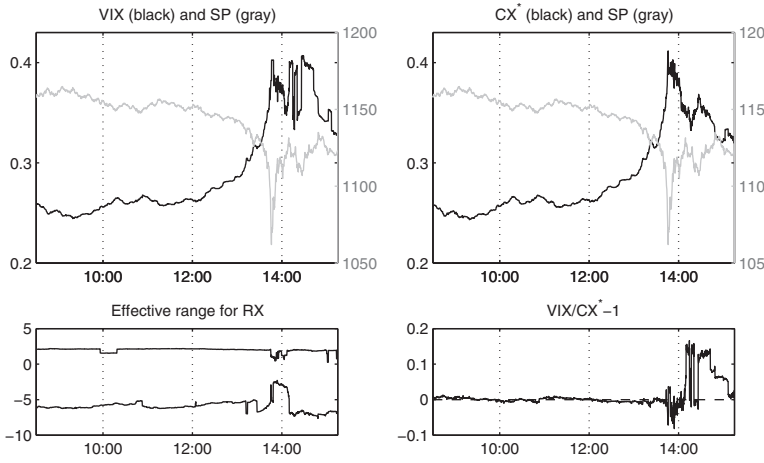

Figure 12
VIX and CX on May 6, 2010
The top panels depict the evolution of the volatility indices (in units given on the left vertical scale) and the S&P 500 futures (in units given on the right vertical scale) across the trading day. The bottom left panel displays the weighted effective strike range used to compute RX, and the bottom right panel conveys the relative discrepancy between the VIX and CX* across the trading day.

the "flash crash." In the CFTC-SEC Report,[34] exploring the market dynamics of this episode, the intraday VIX measure features prominently in the account of the escalating uncertainty gripping the market.

The top left panel of Figure 12 displays the VIX and S&P 500 indices for that trading day. Given the potential problems with VIX during turbulent market conditions, we also plot the S&P 500 series versus a scaled corridor volatility index, CX*. As noted in Section 3.4, the general level of the CX index is effectively proportional to the VIX, whenever the latter is constructed from a stable strike range. We exploit that property to determine the scaling constant which renders CX* nearly identical to VIX between 8:00 and 13:30 on May 6, 2010. The bottom panels of Figure 12 depict the effective strike range for the VIX computation and the relative discrepancy between VIX and CX*.

A number of features in Figure 12 are striking. First, during the early part of the trading day, the VIX and CX* indices are near indistinguishable, and both hit a local peak at the trough of the equity index around 13:46. Second, both decline in erratic fashion over the following 20–25 minutes. Third, the indices then diverge sharply over the next hour, until after 15:00. The VIX spikes up again and attains its maximum around 14:30 while CX* is well below its high of the day. Moreover, the path of the VIX is now characterized by abrupt jumps, while CX* evolves more smoothly, almost as a mirror image of the S&P

[34] *Findings Regarding The Market Events Of May 6, 2010.* Report of the Staffs of the CFTC and SEC to the Joint Advisory Committee on Emerging Regulatory Issues (September 30, 2010). Available at www.sec.gov/news/studies/2010/marketevents-report.pdf.

500 index. Hence, the two series portray vastly different trading environments following the crash. The real-time VIX index conveys a picture of sustained, or even elevated, uncertainty for a prolonged period. The corridor index instead settles down reasonably well around 14:00, and subsequently never reaches a level comparable to the peak at 13:46.

For a real-time observer, the successive VIX spikes in excess of 10% around 14:12 and 14:30 would be rather unsettling. However, the CX* series indicates that these eruptions were fictitious. The stark divergence between the measures is due to features that are, by now, familiar, as we can replicate all major shifts in the VIX from the underlying option quotes and the CBOE truncation rule.[35] Specifically, the bottom left panel reveals dramatic instability in the effective strike range used to compute the VIX both during and in the aftermath of the crash. By construction, our CX measure is robust to such problems. Hence, the relative value of the VIX versus CX*, depicted in the bottom right panel, is indicative of the induced distortions in the VIX. After 13:00, there is a downward drift in the VIX strike range, followed by a period of more pronounced instability, resulting in a downward bias in VIX of up to 5% during the crash phase, succeeded by wild oscillatory swings, producing periodic 10% to 15% overvaluation thereafter. Thus, the VIX is plagued by large artificial shifts. Just as the market conditions deteriorated, the accuracy of the "fear gauge" evaporated.

In summary, the VIX index was severely downward biased at the height of the crash due to collapsing liquidity in the option market. Equally remarkable, the VIX becomes upward biased shortly thereafter, as the effective range expanded beyond the levels seen earlier in the day. The latter likely reflects partial restoration of confidence among market makers and residual customer demand for downside protection after the crash. This results in the VIX attaining its maximum at 14:30, some 45 minutes *after* the market trough. Thus, taking the VIX readings at face value, one may infer, erroneously, that the SPX option prices reacted to the developments with a huge lag. The CX index reverses this finding.

We conclude by quantifying these effects through the equity-index return-volatility correlations. Table 8 shows that all the volatility index returns were strongly negatively correlated with the S&P 500 returns before 13:30, as expected, even if the correlations were the smallest for VIX. These numbers are consistent with the correlations estimated for the full sample in Table 6 so, from this perspective, the market environment was not unusual up to this point. In contrast, after 13:30, except for CX, the correlations shrink dramatically. Hence, only CX retains a near-invariant relation to the underlying S&P 500 index returns throughout the day. Moreover, the values for CX, based on observations covering only a few trading hours, continue to be in line with

[35] In particular, our VIX replication series, RX, basically coincides with VIX and VIX* throughout the entire trading day.

Table 8
Volatility and S&P 500 return correlations, May 6, 2010

	2-min			10-min		
	CX	RX	VIX	CX	RX	VIX
Before 13:30	−0.82	−0.78	−0.65	−0.84	−0.79	−0.78
After 13:30	−0.74	−0.21	−0.15	−0.84	−0.65	−0.43
All	−0.74	−0.23	−0.18	−0.82	−0.65	−0.44

The correlations are reported for volatility indexes CX, RX, and VIX with respect to S&P 500 futures. On this day, the VIX and VIX* indices are identical. The correlations are computed from two- and ten-minute log returns.

the ranges reported in the preceding section, corroborating the claim that we can produce sensible local leverage coefficient estimates via high-frequency returns for our corridor index. Furthermore, consistent with our prior evidence, the officially disseminated VIX series provides the worst coherence with the equity-index throughout the crisis period. The VIX index fails when it is most needed–plagued by large idiosyncratic biases, arising endogenously as turbulence engulfs the markets and frictions grow more prominent.

5. Conclusions

We advocate the use of a directly observable high-frequency corridor implied volatility index, CX, for exploring important features of the underlying return generating process. The approach is essentially model-free and valid under standard no-arbitrage assumptions, as long as the spot volatility and the implied volatility measures are strictly increasing and smooth functions of the state variables. It follows that the corridor volatility index shares important characteristics with the spot volatility process. They jump at the same time, and the sign and relative magnitude of volatility index jumps are indicative of the corresponding features of spot volatility. Likewise, the correlation between the innovations in the corridor volatility index and the equity-index returns are highly informative regarding the corresponding correlation between the returns and spot volatility, that is, the leverage effect.

The point of using the corridor volatility measure, as opposed to the well-known VIX index, is that the high-frequency properties of the VIX are distorted by idiosyncratic shifts in the strike range, inducing artificial jumps into the measure. In contrast, the CX index ensures intertemporal consistency as it covers an economically invariant range of strikes across time. Consequently, the index values may be meaningfully compared across the sample, independently of the liquidity of the options market.

Using this CX index, we establish a number of new results regarding the nature of the high-frequency return dynamics. First of all, the volatility process displays fairly frequent jumps, but the individual jumps are much smaller than one may deduce from daily volatility measures, such as the daily VIX index. Moreover, the volatility jump distribution is largely symmetric and major volatility jumps are accompanied by price jumps of the opposite

sign. We also document a significantly stronger negative spot return-volatility correlation than reported in the extant literature. In addition, the return-volatility asymmetry, or leverage effect, varies systematically with market conditions as it turns increasingly negative when uncertainty grows and return volatility is rising.

Our findings point toward a complex dynamic interaction between the high-frequency return and volatility processes. An improved understanding of these features will help identify the origin of the fat tails and asymmetries that are apparent in longer-horizon return distributions. Moreover, it should be useful for constructing models with a more realistic depiction of the return generating process and thus allow for pricing that incorporate proper risk compensation for the critical factors behind the high-frequency return dynamics and its propagation over longer horizons.

Finally, from a policy perspective, our findings suggest it is beneficial to secure continuous dissemination of a robust implied volatility measures to the marketplace. The main weakness of VIX stems from the cutoff rule applied for the strike range. Empirically, turbulent market conditions are tantamount to wide bid-ask spreads, and they also lead to deteriorating and rapidly shifting liquidity for OTM options. A modification or supplement to the VIX index, exploiting the superior robustness and coherence properties of the corridor index construction, will mitigate this problem. In particular, it will enhance the real-time flow of relevant pricing information during periods of market stress.

Appendix A Theoretical Background

A.1. Proof of Proposition 2

Let $g(F)$ be a general function for which $g''(F)$ is continuous almost everywhere and define $G(F_{i-1},F_i)=2\cdot\left[g(F_i)-g(F_{i-1})-g'(F_{i-1})(F_i-F_{i-1})\right]$. For functions of this general type, Bondarenko (2014) shows that the payoff $\sum_{i=1}^{n}G(F_{i-1},F_i)$ can be robustly replicated, even with jumps. In particular, it follows from his Proposition 4 and Corollary 1 that the model-free price of this payoff is given by

$$E_0^{\mathbb{Q}}\left[\sum_{i=1}^{n}G(F_{i-1},F_i)\right]=2\int_0^{\infty}g''(K)M_0(K)dK. \tag{A.1}$$

To apply this result, we choose $g(F)=1-\ln\frac{F}{\overline{F}}-\frac{F}{\overline{F}}$, where $\overline{F}$ is defined in Equation (9). It is easy to verify that $g(F)$ has a continuous second derivative everywhere, except at B_L and B_H. In particular,

$$g'(F)=-\frac{1}{\overline{F}},\qquad g''(F)=\frac{1}{F^2}I(F;B_L,B_H).$$

The corresponding function $G(F_{i-1},F_i)$ can be simplified as,

$$G(F_{i-1},F_i)=2\left(\frac{F_i}{\overline{F}_i}\left(\frac{\overline{F}_i-\overline{F}_{i-1}}{\overline{F}_{i-1}}\right)-\ln\frac{\overline{F}_i}{\overline{F}_{i-1}}\right)=\left(\bar{r}_i^{w}\right)^2. \tag{A.2}$$

The definition of the corridor realized variance CRV^w in Equation (11), together with Equation (A.1), then imply

$$E_0^{\mathbb{Q}}\left[CRV^w\right]=E_0^{\mathbb{Q}}\left[\sum_{i=1}^{n}G(F_{i-1},F_i)\right]=2\int_{B_L}^{B_H}\frac{M_0(K)}{K^2}dK.$$

■

A.2. Continuous-Time Limits

In the continuous-time limit, as $\Delta t \to 0$, the realized variances in Equations (4) and (6) converge to the following three version of the quadratic variation:

$$RV^w \to QV^w = \int_0^T v_t\,dt + \sum_{0\le s<T} 2(\kappa_s - \ln(1+\kappa_s)) \;=\; IV + JV^w,$$

$$RV^c \to QV^c = \int_0^T v_t\,dt + \sum_{0\le s<T} [\ln(1+\kappa_s)]^2 = IV + JV^c,$$

$$RV^s \to QV^s = \int_0^T v_t\,dt + \sum_{0\le s<T} \kappa_s^2 = IV + JV^s.$$

The three quadratic variations QV^w, QV^c, and QV^s differ only with regard to how they treat jumps. When there are no jumps, they all coincide with the integrated variation IV.

Similarly, the corridor realized variance CRV^w converges to the corridor quadratic variation:

$$CRV^w \to CQV^w = \int_0^T v_t\, I(F_t; B_L, B_H)dt + \sum_{0\le s\le T} G(F_s, F_s(1+\kappa_s)), \tag{A.3}$$

where G is defined in (A.2), F_s denotes the price before jump κ_s, and $I(F; B_L, B_H) = 1[B_L \le F \le B_H]$ is the indicator function, taking the value of unity if the price is within $[B_L, B_H]$, and zero otherwise. The first term on the right-hand side is the corridor integrated variance, and the second term is the corridor jump variation.

Appendix B Extracting Forward Prices from the Option Surface

The forward price, F, and the strike price just below the forward price, K_f, enter in Equation (13), but they are not directly observable. The CBOE determines these basic variables from the available option quotes in three steps. First, for each maturity separately, the strike price K^* for which the distance between the quoted midpoints of the call and put prices is minimal is identified. This strike is then used to compute the "implied" forward according to put-call parity, $F^* = K^* + e^{rT} \times [C(K^*, T) - P(K^*, T)]$. Finally, K_f is determined as the first available strike price below F^*.

Our analysis established that this feature of the CBOE methodology entails a certain lack of robustness, arising from the use of only a single (K^*) put-call option price pair to infer F^* and K_f. Occasional problems, like a temporary gap in the quote updating for a subset of options or a basic recording error, can cause the minimum distance between the call and put prices to erroneously appear at a point far from the true ATM strike. In turn, this can generate a large bias in the VIX and may even render its computation infeasible.

Motivated by this observation, we develop a more robust procedure for determining the implied forward. In a first step, for the given maturity, we identify the set of strikes for which the discrepancy between the price of the put and call is below \$25. Second, for each of these put-call option pairs, we compute the implied forward price. Third, we designate the "robust implied forward" as the median of this set of implied forward prices. Using a robust statistic defined over multiple option pairs prunes the implied forward series of major erroneous outliers. On the other hand, the wider set may include less liquid options with large relative spreads or pricing errors. Consequently, as our final step, we retain the original F^* value, rather than the robust forward, unless the two values differ substantially. Following diagnostic checks, we chose a relative threshold of 0.5%.[36] Hence,

[36] For a level of the S&P 500 around 1,000, the threshold is about five, which is the same order of magnitude as the gap between the strike prices.

if the two implied forwards are close, we stick with F^*, but if they differ by more than 0.5%, we instead adopt the robust implied forward. This procedure generates an implied forward price, F, that typically coincides with F^*, but deviates whenever F^* may contain a sizeable error.

Appendix C Data and Data Filtering

C.1. The SPX Option Classes

We acquired the Market Data Retrieval (MDR) data for S&P 500 options from the CBOE subsidiary, Market Data Express (www.marketdataexpress.com/). The MDR data include tick-by-tick quotes and transactions throughout the trading day for all option classes issued by the CBOE on the S&P 500. Each option class is characterized by a letter code. We only consider options that the CBOE actually used in their computation of the VIX over our sample period, namely, those in the SPB, SPQ, SPT, SPV, SPX, SPZ, SVP, SXB, SXM, SXY, SXZ, SYG, SYU, SYV, and SZP categories. The latter are generally known as SPX equity options, and they mature on the Saturday immediately following the third Friday of the expiration month (see www.cboe.com/Products/EquityOptionSpecs.aspx).

C.2. Systemic Staleness in Option Quotes

By far, the most influential options for the computation of model-free implied volatility measures are put and call options with strikes close to the at-the-money (ATM). Hence, we actively monitor the liquidity of the set of twenty OTM put and twenty OTM call options closest to the forward price for the two maturities exploited for the VIX computation. We label this group of options the "pivotal" ones.

Our filter for systemic staleness is designed to flag periods in which problems in the quote dissemination system may induce nontrivial errors in the volatility index calculations. Specifically, the filter assigns a value of unity to an associated dummy variable, if there are no quote updates for all the options within one of our four pivotal option categories over a five-minute period, and zero otherwise. When the flag is activated (equals unity), we classify the entire inactive period of five minutes or more as unreliable, and the volatility indices are not available (n.a.).

C.3. The Nonconvexity Filter

To preclude arbitrage opportunities, theoretical call and put prices must be monotonic and convex functions of the strike. In particular, the call prices must satisfy the following convexity restriction:

$$D_i = \frac{C(K_{i+1}) - C(K_i)}{K_{i+1} - K_i} - \frac{C(K_i) - C(K_{i-1})}{K_i - K_{i-1}} \geq 0,$$

and a similar restriction for the put prices. We obtain the option prices as the average of the bid and ask quotes and use the above restriction to identify "suspect" cross-sections with apparent arbitrage violations, which could arise from recording errors, staleness, and other issues. Specifically, for each strike K_i, we compute a measure of local nonconvexity, defined as $NC_i = -\min\{D_i, 0\}$. For low strikes ($K_i \leq F$), we compute NC_i from OTM puts and, for high strikes ($K_i > F$), we use OTM calls. We then average NC_i across all strikes to obtain the aggregate measure of nonconvexity NC.

When $NC > 0.1$, we deem a cross-section as unreliable and do not use it in our econometric analysis. For those cross-sections, the option prices indicate sizeable apparent arbitrage opportunities. However, for some illustrations, we need to compute volatility indices even when the quality of data is poor ($NC > 0.1$). In those cases, prior to computing the volatility indices, we adjust option prices by running the so-called Constrained Convex Regression (CCR). This procedure has been implemented in Bondarenko (2000). Intuitively, CCR searches for the smallest (in the sense of least squares) perturbation of option prices that restores the no-arbitrage restrictions.

C.4. The Bounce-Back Filter

We detect situations in which a volatility index experiences a large move, which is almost immediately offset by a jump of a similar magnitude, but in the opposite direction. Such behavior is usually indicative of a data error that impacts only a few recorded quotes. Such an error induces a jump in returns when it occurs and then another one when the error is eliminated and the recorded quotes reverse to their appropriate level. Specifically, we label such incidents as " bouncebacks" if the index jumps by at least nine "sigmas" and either (1) more than 75% of this jump is reversed within one minute or (2) more than 80% of the jump is reversed within two minutes.

Appendix D Robust Volatility Estimation

For a given volatility index, let the associated one-minute log return at time t on trading day d be r_{dt}. We assume this return may be represented as

$$r_{dt} = \sigma_d f_t z_{dt},$$

where σ_d is average volatility for trading day d, f_t is a scaling factor which adjusts for the intraday volatility pattern, and z_{dt} are i.i.d., potentially nonnormal, random variables with zero mean and unit standard deviation.

We estimate the daily volatilities $\{\sigma_d\}_1^{N_d}$ and intraday adjustment factors $\{f_t\}_1^{N_t}$ as follows. First, for fixed t, we compute the average squared return across all trading days,

$$\frac{1}{N_d}\sum_d^{N_d} r_{dt}^2 = f_t^2 \cdot \frac{1}{N_d}\sum_d^{N_d} \sigma_d^2 z_{dt}^2.$$

Since z_{dt} are i.i.d. with $E[z_{dt}]=0$ and $\mathrm{Var}(z_{dt})=1$, we obtain,

$$E\left[\frac{1}{N_d}\sum_d^{N_d} r_{dt}^2\right] = f_t^2 \cdot \left(\frac{1}{N_d}\sum_d^{N_d}\sigma_d^2\right) = V_{mean}\cdot f_t^2,$$

where V_{mean} is a constant independent of t. Therefore, the adjustment factor f_t may be estimated as

$$f_t^2 = \frac{\frac{1}{N_d}\sum_d^{N_d} r_{dt}^2}{V_{mean}},$$

where V_{mean} now is determined from the condition that,

$$\sigma_d^2 = \frac{1}{N_t} E\left[\sum_t^{N_t} r_{dt}^2\right] = \frac{1}{N_t}\sum_t^{N_t}\sigma_d^2 \cdot f_t^2,$$

or

$$\frac{1}{N_t}\sum_t^{N_t} f_t^2 = 1. \tag{A.4}$$

The above approach provides an unbiased estimator of f_t^2. However, it might not be robust in the presence of extreme returns in the r_{dt} series. Therefore, we implement a robustified version of the same approach, based on the sample median rather than the mean. Specifically,

$$E\left[\mathrm{Median}_d\left\{r_{dt}^2\right\}\right] = f_t^2 \mathrm{Median}_d\left\{\sigma_d^2\right\} = V_{med}\cdot f_t^2,$$

where V_{med} again denotes a constant independent of t. The adjustment factor f_t is then estimated as

$$f_t^2 = \frac{\mathrm{Median}_d\left\{r_{dt}^2\right\}}{V_{med}},$$

subject to the constraint in Equation (A.4). For additional robustness, the estimated intraday factors are smoothed by averaging them over ten-minute windows.[37] Armed with $\{f_t\}_1^{N_t}$, the

[37] For all volatility indices, the intraday factors range from about 0.6 to 2.0.

daily volatility σ_d can now be estimated as the volatility of the re-scaled returns, $u_{dt} = \frac{r_{dt}}{f_t}$. This could be done in many ways, but we focus on the robust estimator based on the 5th to 95th percentile range. Specifically, we sort the rescaled returns u_{dt} for a given day d and determine their 5th and 95th percentiles, $P(0.05)$ and $P(0.95)$. Then

$$\sigma_d = \frac{P(0.95) - P(0.05)}{3.2898},$$

where the denominator equals the 5th to 95th percentile range of the standard normal random variable.[38]

Finally, when defining large index returns, we take into account both the daily measure of volatility σ_d and the intraday adjustment factor f_t. That is, the move is deemed large if the absolute value of the ratio

$$\left| \frac{r_{dt}}{\sigma_d f_t} \right| = \left| \frac{u_{dt}}{\sigma_d} \right|$$

exceeds a prespecified threshold.

References

Aït-Sahalia, Y., J. Fan, and Y. Li. 2013. The leverage effect puzzle: Disentangling sources of bias at high frequency. *Journal of Financial Economics* 109:224–49.

Albuquerque, R. 2012. Skewness in stock returns: reconciling the evidence on firm versus aggregate returns. *Review of Financial Studies* 25:1630–73.

Amengual, D., and D. Xiu. 2014. Resolution of policy uncertainty and sudden declines in volatility. Working Paper, University of Chicago.

Andersen, T. G., and O. Bondarenko. 2007. Construction and interpretation of model-free implied volatility. In *Volatility as an Asset Class*. Ed. I. Nelken, 141–81. London: Risk.

———. 2013. Dissecting the pricing of equity index volatility. Working Paper, Northwestern University, and University of Illinois at Chicago.

———. 2015. Assessing measures of order flow toxicity and early warning signals for market turbulence. *Review of Finance* 19:1–54.

Andersen, T. G., O. Bondarenko, and M. T. Gonzalez-Perez. 2015. A corridor fix for high-frequency vix: developing coherent implied volatility measures. Working Paper, Northwestern University, University of Illinois at Chicago, and CUNEF.

Bandi, F. M., and R. Reno. 2012. Time-varying leverage effects. *Journal of Econometrics* 169:94–113.

———. 2015 forthcoming. Price and volatility co-jumps. *Journal of Financial Economics*.

Bekaert, G., and G. Wu. 2000. Asymmetric volatility and risk in equity markets. *Review of Financial Studies* 13:1–42.

Black, F. 1976. Asset pricing for general processes. *Proceedings of the 1976 Meetings of the American Statistical Association* 1976:171–81.

Bondarenko, O. 2000. Recovering risk-neutral densities: A new nonparametric approach. Working Paper, University of Illinois at Chicago.

———. 2014. Variance trading and market price of variance risk. *Journal of Econometrics* 180:81–97.

Britten-Jones, M., and A. Neuberger. 2000. Option prices, implied price processes, and stochastic volatility. *Journal of Finance* 55:839–66.

[38] We also experimented with other robust estimators of σ_d, and the results are quantitatively similar.

Broadie, M., M. Chernov, and M. Johannes. 2007. Model specification and risk premia: Evidence from futures options. *Journal of Finance* 62:1453–90.

Campbell, J. Y., and L. Hentschel. 1992. No news is good news: An asymmetric model of changing volatility in stock returns. *Journal of Financial Economics* 31:281–318.

Carr, P., R. Lee, and L. Wu. 2012. Variance swaps on time-changed levy processes. *Finance and Stochastics* 16:335–55.

Carr, P., and D. B. Madan. 1998. Option valuation using the fast fourier transform. *Journal of Computational Finance* 2:61–73.

Carr, P., and L. Wu. 2009. Variance risk premiums. *Review of Financial Studies* 22:1311–41.

Christie, A. A. 1982. The stochastic behavior of common stock variances: Value, leverage and interest rate effects. *Journal of Financial Economics* 10:407–32.

Duffee, G. R. 1995. Stock returns and volatility: A firm-level analysis. *Journal of Financial Economics* 37:399–420.

Easley, D., M. L. de Prado, and M. O'Hara. 2012. Flow toxicity and liquidity in a high-frequency world. *Review of Financial Studies* 25:1457–93.

Engle, R. F., and V. Ng. 1993. Measuring and testing the impact of news in volatility. *Journal of Finance* 48:1749–78.

Eraker, B., M. Johannes, and N. Polson. 2003. The impact of jumps in volatility and returns. *Journal of Finance* 58:1269–300.

French, K. R., G. W. Schwert, and R. F. Stambaugh. 1987. Expected stock returns and volatility. *Journal of Financial Economics* 19:3–29.

Glosten, L. R., R. Jagannathan, and D. E. Runkle. 1993. On the relationship between the expected value and the volatility of the nominal excess return on stocks. *Journal of Finance* 48:1779–802.

Harvey, C. R., and A. Siddique. 2000. Time-varying conditional skewness and the market risk premium. *Research in Banking and Finance* 1:25–58.

Ishida, I., M. McAleer, and K. Oya. 2011. Estimating the leverage parameter of continuous-time stochastic volatility models using high-frequency s&p 500 and vix. *Managerial Finance* 37:1048–67.

Jacod, J., and M. Rosenbaum. 2013. Quarticity and other functionals of volatility: Efficient estimation. *Annals of Statistics* 41:1462–84.

Jacod, J., and V. Todorov. 2010. Do price and volatility jump together? *Annals of Applied Probability* 20:1425–69.

Jiang, G. J., and R. C. A. Oomen. 2008. Testing for jumps when asset prices are observed with noise a "swap variance" approach. *Journal of Econometrics* 144:352–70.

Jiang, G. J., and Y. S. Tian. 2005. The model-free implied volatility and its information content. *Review of Financial Studies* 18:1305–42.

Kalnina, I., and D. Xiu. 2014. Nonparametric estimation of the leverage effect using information from derivatives markets. Working Paper, University of Montreal and Booth School, University of Chicago.

Martin, I. 2012. Simple variance swaps. Working Paper, Stanford University.

Nagel, S. 2012. Evaporating liquidity. *Review of Financial Studies* 25:2005–39.

Nelson, D. B. 1991. Conditional heteroskedasticity in asset returns: A new approach. *Econometrica* 59:347–70.

Todorov, V., and G. Tauchen. 2011. Volatility jumps. *Journal of Business and Economic Statistics* 29:356–71.

Wang, D. C., and P. A. Mykland. 2014. The estimation of leverage effect with high frequency data. *Journal of the American Statistical Association* 109:197–215.